ability of NSCs from $NPC^{-/-}$ was recovered when cells were treated with SB202190, p38 MAPK inhibitor but not PD 98059, pERK kinase inhibitor. These data suggest that hyperactivation of MKK3/6, p38 MAPK but not ERK1/2 might be related to generation and differentiation of NSCs from $NPC1^{-/-}$ mice. This is evidence for the possibility that there is a link between the lack of self-renewal of NSCs and some of the neuropathological symptoms seen in NPC1 patients. Thus, anti-MAPK agents could be of therapeutic importance in patients with the NPC1 disorder.

Astrocytes are considered a most important part of neurogenesis, which regulates synapse formation and synaptic transmission, reinforcing the emerging view that astrocytes have an active regulatory role rather than merely supportive roles traditionally assigned to them in the mature CNS [32]. Suzuki et al. [33] reported that neuropathologic alterations of astrocytes are presented in NPC1 disease. Consistent with this, the absence of NPC1 gene leads to a significant number of different phenotypes of astrocytes when NSCs from $NPC^{-/-}$ mice are differentiated. We suggest that these morphologically altered astrocytes are due to the deficiency of NPC1 gene through the activation of the p38 MAPK. Thus, NPC1 deficiency leads to lack of self-renewal ability and altered morphology of astrocytes through the activation of p38 MAPK, suggesting that p38 MAPK inhibitors may be an effective method for increasing self-renewal of NSCs for clinical application in NPC1 disease. It is clear that a greater understanding of the exact mechanism of self-renewal and the function of the NPC1 protein should provide better insights into the application of stem cell therapy in neurodegenerative diseases. We conclude that the NPC1 gene may be a candidate gene for controlling self-renewal of NSCs throughout life.

ACKNOWLEDGMENTS

This work was supported by a grant from the Korean Science & Engineering Foundation (R01-2005-000-10190-0) and a grant from the Korean Research Foundation (KRF-005-E00076).

DISCLOSURES

The authors indicate no potential conflicts of interest.

REFERENCES

1 Storch A, Schwarz J. Neural stem cells and Parkinson's disease. J Neurol 2002;249(suppl 3):30-32.

2 McBride JL, Behrstock SP, Chen EY et al. Human neural stem cell transplants improve motor function in a rat model of Huntington's disease. J Comp Neurol 2004;475:211–219.

3 Artavanis-Tsakonas S, Matsuno K, Fortini ME. Notch signaling. Science 1995;268:225–232.

4 Zilian O, Saner C, Hagedorn L et al. Multiple roles of mouse Numb in tuning developmental cell fates. Curr Biol 2001;11:494–501.

5 Oishi K, Kamakura S, Isazawa Y et al. Notch promotes survival of neural precursor cells via mechanisms distinct from those regulating neurogenesis. Dev Biol 2004;276:172–184.

6 Chitnis AB. The role of Notch in lateral inhibition and cell fate specification. Mol Cell Neurosci 1995;6:311–321.

7 Morrison SJ, Perez SE, Qiao Z et al. Transient Notch activation initiates an irreversible switch from neurogenesis to gliogenesis by neural crest stem cells. Cell 2000:101:499–510.

8 Roegiers F, Jan YN. Asymmetric cell division. Curr Opin Cell Biol 2004;16:195–205.

9 Berdnik D, Torok T, Gonzalez-Gaitan M et al. The endocytic protein α-Adaptin is required for Numb-mediated asymmetric cell division in Drosophila. Dev Cell 2002;3:221–231.

10 Fukuda S, Taga T. Cell fate determination regulated by a transcriptional signal network in the developing mouse brain. Anat Sci Int 2005;80:12–18.

11 Corson LB, Yamanaka Y, Lai KM et al. Spatial and temporal patterns of ERK signaling during mouse embryogenesis. Development 2003;130: 4527–4537.

12 Zhang W, Liu HT. MAPK signal pathways in the regulation of cell proliferation in mammalian cells. Cell Res 2002;12:9–18.

13 Yang SR, Cho SD, Ahn NS et al. The role of p38 MAP kinase and c-Jun N-terminal protein kinase signaling in the differentiation and apoptosis of immortalized neural stem cells. Mutat Res 2005;579:47–57.

14 Yang SR, Cho SD, Ahn NS et al. Role of gap junctional intercellular communication (GJIC) through p38 and ERK1/2 pathway in the differentiation of rat neuronal stem cells. J Vet Med Sci 2005:67:291–294.

15 Xia Z, Dickens M, Raingeaud J et al. Opposing effects of ERK and JNK-p38 MAP kinases on apoptosis. Science 1995;270:1326–1331.

16 Zhao WQ, Alkon DL, Ma W. c-Src protein tyrosine kinase activity is required for muscarinic receptor-mediated DNA synthesis and neurogenesis via ERK1/2 and c-AMP-responsive element-binding protein signaling in neural precursor cells. J Neurosci Res 2003;72:334–342.

17 Cruz JC, Chang TY. Fate of endogenously synthesized cholesterol in Niemann-Pick type C1 cells. J Biol Chem 2000;275:41309–41316.

18 Cruz JC, Sugii S, Yu C et al. Role of Niemann-Pick type C1 protein in intracellular trafficking of low density lipoprotein-derived cholesterol. J Biol Chem 2000;275:4013–4021.

19 Griffin LD, Gong W, Verot L et al. Niemann-Pick type C disease involves disrupted neurosteroidogenesis and responds to allopregnanolone. Nat Med 2004;10:704–711.

20 Sun X, Marks DL, Park WD et al. Niemann-Pick C variant detection by altered sphingolipid trafficking and correlation with mutations within a specific domain of NPC1. Am J Hum Genet 2001;68:1361–1372.

21 Loftus SK, Morris JA, Carstea ED et al. Murine model of Niemann-Pick C disease: Mutation in a cholesterol homeostasis gene. Science 1997; 277:232–235.

22 Ory DS. Niemann-Pick type C: A disorder of cellular cholesterol trafficking. Biochim Biophys Acta 2000;1529:331–339.

23 Carstea ED, Morris JA, Coleman KG et al. Niemann-Pick C1 disease gene: Homology to mediators of cholesterol homeostasis. Science 1997; 277:228–231.

24 Sawamura N, Gong JS, Garver WS et al. Site-specific phosphorylation of tau accompanied by activation of mitogen-activated protein kinase (MAPK) in brains of Niemann-Pick type C mice. J Biol Chem 2001; 276:10314–10319.

25 Ullian EM, Sapperstein SK, Christopherson KS et al. Control of synapse number by glia. Science 2001:291:657–661.

26 Mauch DH, Nagler K, Schumacher S et al. CNS synaptogenesis promoted by glia-derived cholesterol. Science 2001;294:1354–1357.

27 Patel SC, Suresh S, Kumar U et al. Localization of Niemann-Pick C1 protein in astrocytes: Implications for neuronal degeneration in Niemann-Pick type C disease. Proc Natl Acad Sci U S A 1999:96:1657–1662.

28 Levy YS, Stroomza M, Melamed E et al. Embryonic and adult stem cells as a source for cell therapy in Parkinson's disease. J Mol Neurosci 2004;24:353–386.

29 Dunnett SB, Rosser AE. Cell therapy in Huntington's disease. Neurorx 2004;1:394–405.

30 Burns M, Gaynor K, Olm V et al. Presenilin redistribution associated with aberrant cholesterol transport enhances beta-amyloid production in vivo. J Neurosci 2003;23:5645–5649.

31 Molofsky AV, Pardal R, Iwashita T et al. Bmi-1 dependence distinguishes neural stem cell self-renewal from progenitor proliferation. Nature 2003;425:962–967.

32 Song H, Stevens CF, Gage FH. Astroglia induce neurogenesis from adult neural stem cells. Nature 2002;417:39–44.

33 Suzuki H, Sakiyama T, Harada N et al. Pathologic changes of glial cells in murine model of Niemann-Pick disease type C: immunohistochemical, lectin-histochemical and ultrastructural observations. Pediatr Int 2003: 45:1–4.

NPC1 Gene Deficiency Leads to Lack of Neural Stem Cell Self-Renewal and Abnormal Differentiation Through Activation of p38 Mitogen-Activated Protein Kinase Signaling

Se-Ran Yang, Sun-Jung Kim, Kyoung-Hee Byun, Brian Hutchinson, Bong-Hee Lee, Makoto Michikawa, Yong-Soon Lee and Kyung-Sun Kang

Stem Cells 2006;24;292-298; originally published online Aug 11, 2005;
DOI: 10.1634/stemcells.2005-0221

Acta Neurol Scand 2006: 114 (Suppl. 185): 21–26

ACTA NEUROLOGICA
SCANDINAVICA

Role of cholesterol in amyloid cascade: cholesterol-dependent modulation of tau phosphorylation and mitochondrial function

Michikawa M. Role of cholesterol in amyloid cascade: cholesterol-dependent modulation of tau phosphorylation and mitochondrial function. Acta Neurol Scand 2006: 114 (Suppl. 185): 21–26. © Blackwell Munksgaard 2006.

Apolipoprotein E (apoE) alleles are important genetic risk factors for Alzheimer's disease (AD), with the ε4 allele increasing and the ε2 allele decreasing the risk of developing AD. ApoE is the major apolipoprotein that modulates cholesterol transport in the central nervous system, cholesterol being an essential component of membranes for maintaining their structure and functions. Epidemiological studies have suggested a link between serum cholesterol levels and AD development and the potential therapeutic effectiveness of statins for AD; and furthermore, biological studies have shown that amyloid β-protein (Aβ) secretion is modulated by cellular cholesterol level. However, other lines of evidence show controversial results. In addition to the role of cholesterol in Aβ generation, different interactions of cholesterol with Aβ and its role in AD pathogenesis have been shown, i.e. Aβ affects cholesterol dynamics in neurons, and altered cholesterol metabolism in turn leads to neurodegeneration with abnormally phosphorylated tau (tauopathy). In this review, the reciprocal interactions between cholesterol and Aβ, and the role of cholesterol in tauopathy are discussed. The isoform-specific involvement of apoE in this cascade, in which high-density lipoprotein-like particles are generated and supplied to neurons to maintain cholesterol homeostasis, is also discussed.

M. Michikawa

Department of Alzheimer's Disease Research, National Institute for Longevity Sciences, Aichi, Japan

Key words: Alzheimer's disease; amyloid β-protein; apolipoprotein E; cholesterol; high-density lipoprotein; Niemann–Pick type C1 disease; statin; tau phosphorylation

Makoto Michikawa, Department of Alzheimer's Disease Research, National Institute for Longevity Sciences, 36-3 Gengo, Morioka, Obu, Aichi 474-8522, Japan
Tel.: +81 562 46 2311
Fax: +81 562 46 3157
e-mail: michi@nils.go.jp

Accepted for publication 16 April, 2006

Cholesterol transport system in central nervous system

Studies of cholesterol metabolism in the systemic circulation have been performed for decades. However, knowledge of the cholesterol transport system in the central nervous system (CNS), the most lipid-rich organ that accounts for 20–25% of the total body cholesterol, is very limited. As CNS is segregated by the blood–brain barrier from the systemic circulation, the regular lipid transport system mediated by plasma lipoproteins is not generally available. Accordingly, the cholesterol transport in the CNS is postulated to be regulated independent of the systemic circulation. For example, several types of lipoproteins are identified in the systemic circulation including chylomicrons, very low-density lipoproteins (VLDL), low-density lipoproteins (LDL), intermediate-density lipoproteins (IDL), and high-density lipoproteins (HDL), whereas only HDL-like lipoproteins are found in the cerebrospinal fluid (CSF) (1, 2). Demonstration that the original apolipoprotein E (apoE) phenotype of a recipient in the CNS remained unchanged even after liver transplantation, which changed the plasma apoE phenotype (3), suggests that apoE in the CSF is produced within the CNS and is unexchangeable with the apoE associated with the plasma lipoproteins.

Under conditions in which cholesterol supply from the blood is not available, how do neurons obtain cholesterol? To answer this fundamental question, previous studies have shown a new type of neuron–glia interaction in the CNS, by which cholesterol is supplied to neurons for synapse formation and neurite outgrowth. It has been shown that cholesterol is a synapse-promoting

factor secreted from glia cells in apoE-containing lipoproteins (4), and that glial-derived lipoproteins containing apoE stimulate axon extension (5). In accordance with these findings, glial cells produce two- to threefold more cholesterol than neurons and secrete it as apoE-lipoprotein particles (6, 7), which are supplied to neurons via apoE receptors. The morphology of neurons is quite different from that of other cells in that neurons have a large number of long complicated processes, which have a membrane area 10- to 100-fold that of the cell body (8). In addition, more than 20% of the clusters of post-synaptic densities turn over within 24 h in hippocampal neurons (9). These may explain why neurons import cholesterol rather than synthesize it, which would require them to have a whole battery of enzymes distributed in different subcellular organelles and to consume large amounts of energy substrates.

Association of serum total and LDL cholesterol levels with risk of Alzheimer's disease: why and how?

Recent epidemiological studies have revealed the plausibility of a link between Alzheimer's disease (AD) and cholesterol metabolism based on the associations of an elevated serum total cholesterol level with a high prevalence of AD and mild cognitive impairment (MCI) (10, 11). These associations correlate well with the finding that the apoE allele ε4 is a strong risk factor for AD development, because there is a stepwise increase, as a function of alleles (ε2 to ε3 to ε4), in serum total and LDL cholesterol levels (12–16). The decreased prevalence of AD in individuals treated with statins (17) seems to strengthen this notion. Although the cause and effect relationship between high serum cholesterol levels and enhanced Aβ generation or secretion has not yet been demonstrated, another explanation has been proposed, i.e. a decreased cellular cholesterol level suppresses the synthesis of Aβ in neurons (18) and the secretion of Aβ from cells into the CSF *in vivo* (19). These lines of evidence imply that increased levels of serum total cholesterol and LDL cholesterol lead to an increased cellular cholesterol level in the CNS through the blood–brain barrier. However, the relationship between cholesterol levels in serum and in the CSF or CNS has not yet been established, and this notion has been partly challenged by recent studies showing that a reduced cholesterol level in detergent-resistant membrane domains of AD brains (20) and that a slight decrease in cellular cholesterol levels enhance Aβ generation (21). All these results indicate that major issues still remain to be resolved as follows: how cholesterol metabolism in the CNS and in the systemic circulation are associated beyond the blood–brain barrier; how cholesterol metabolism within the CNS is regulated; and how altered cholesterol metabolism in neurons or glia cells is associated with AD development and progression.

Relationship between serum and CSF cholesterol levels

The most fundamental and thus critical concern is that there is currently no explanation for how serum cholesterol levels are involved in brain diseases beyond the blood–brain barrier. Therefore, the above-mentioned data must be interpreted with caution and several issues need to be resolved before the idea that high serum cholesterol levels and, if it is the case, high cholesterol levels in CNS cells are responsible for AD development can be fully accepted. It has been shown that there is no significant correlation between CSF and serum cholesterol levels (22, 23), and that serum cholesterol level has no effect on the level of HMG-CoA reductase mRNA and its activity in the brain (24). These lines of evidence cannot explain why significantly higher levels of serum total cholesterol lead to a higher prevalence of AD, because of the differences between serum and CNS cholesterol metabolism.

Association of plasma HDL cholesterol level with risk of AD

If serum total and LDL cholesterol levels have no correlation with CSF cholesterol levels, does it mean that CNS cholesterol is not involved in AD pathogenesis? Thus, I propose an alternative interpretation of previous data. In previous reports, the authors mainly discussed the relationship between serum cholesterol levels and AD development; they did not focus on HDL cholesterol levels (10, 11, 25, 26). As has been reported, the LDL and total cholesterol levels are highest in those with apoE4, intermediate in those with apoE3 and lowest in those with apoE2 (12–16). However, it has also been shown that HDL cholesterol levels are highest in those with apoE2, intermediate in those with apoE3 and lowest in those with apoE4 (14–16), which can be explained by the isoform-dependent apoE ability to release cholesterol from cells to generate HDL particles (27, 28). This apoE-isoform-dependent HDL cholesterol level is also found in AD patients in whom serum HDL cholesterol levels inversely correlate with the dose of the apoE allele ε4 (29). It has also been shown that serum HDL cholesterol levels of AD patients is lower than that of controls,

decreased serum HDL cholesterol levels being correlated with AD severity (30), and HDL cholesterol levels are lower in the CSF of AD patients than in that of controls (31). A previous study showed that there is a strong correlation between CSF and serum HDL cholesterol levels, but not between CSF and serum total or LDL cholesterol levels (22). These lines of evidence led us to hypothesize that a low cholesterol level in serum and CSF is a risk factor for AD development. In accordance with this notion, recent studies have shown that cholesterol level decreases in the white matter (32) and detergent-resistant membrane domains (20) of AD brains. Moreover, a slight reduction in cellular cholesterol levels has been demonstrated to enhance Aβ generation (21). These results are contrary to what had been reported and accepted, indicating that further studies are required to better understand how lipoprotein cholesterol levels are associated with AD pathogenesis including Aβ generation or secretion.

Role of cholesterol in amyloid cascade

Oligomeric Aβ impairs cholesterol metabolism in neurons

How is altered cholesterol metabolism involved in AD pathogenesis? Previous studies have focused on cholesterol-mediated Aβ synthesis. However, here, I propose a different notion explaining the role of cholesterol in the amyloid cascade by promoting AD pathologies as follows: with respect to the neurotoxic effect of Aβ, it is widely accepted that oligomerization is a critical step for Aβ to impair neuronal functions (33). We have also found that Aβ, when it forms oligomers, affects cholesterol metabolism in neurons. Oligomeric Aβ causes cholesterol and phospholipid release to generate an Aβ–lipid complex whose density is similar to that of HDL. This Aβ–lipid complex is not taken up by neurons, whereas HDL generated by apoE can be taken up via apoE receptors and used by neurons (34). In addition, the oligomeric Aβ impairs cholesterol synthesis and finally reduces cholesterol levels in neurons (35). In contrast, Aβ monomers do not have such an effect; rather, they have a strong neuroprotective function as radical scavengers (36) (Fig. 1B).

Decreased cellular cholesterol levels promote tau phosphorylation and impair mitochondrial functions

Aβ-mediated alteration in cellular cholesterol homeostasis presumably leads to synaptic dysfunction, because cholesterol levels in neurons, derived

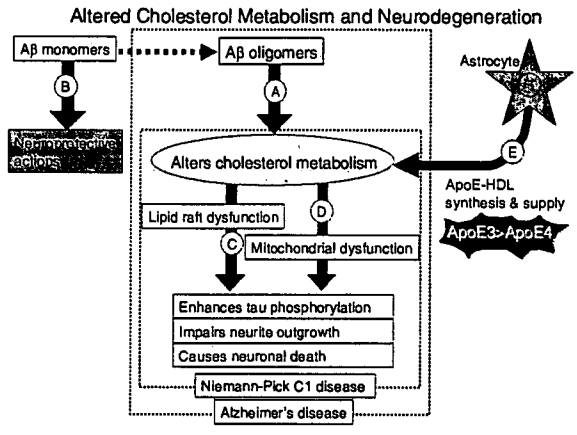

Figure 1. Hypothetical schema showing putative role of cholesterol in amyloid cascade that promotes AD pathogenesis. Increased extracellular Aβ levels with aging result in the formation of soluble oligomers and insoluble assemblies such as fibrils. (A) Oligomeric Aβ has been shown to affect cholesterol metabolism in neurons and to finally reduce cellular cholesterol levels in neurons by promoting cholesterol release from neurons to generate HDL–Aβ complexes (34), inhibiting cholesterol synthesis (35). (B) In contrast, Aβ monomers protect neurons (36). (C) The disruption of cholesterol homeostasis in neuronal membranes caused by oligomeric Aβ may induce AD pathological alterations including enhanced tau phosphorylation (38, 39), inhibition of dendrite outgrowth (37), impairment of synaptogenesis and synaptic plasticity (4, 5), and neurodegeneration (38, 52). (D) Interestingly, an altered cholesterol level in the mitochondrial membrane impairs mitochondrial functions, which results in a reduced cellular ATP level in neurons (47). (E) ApoE is involved in this cascade as an HDL generator and an HDL cholesterol supplier to neurons via apoE receptors in an apoE-isoform-dependent manner (27, 28).

from glial cells as apoE-containing lipoproteins, have been shown to play a critical role in the formation of mature synapses (4) and in neurite outgrowth (5, 37). Our findings and that of others suggest that cellular cholesterol levels modulate neurite outgrowth by modulating cellular kinases and phosphatases, and a decrease in cholesterol levels result in a dendrite-specific inhibition of neurite outgrowth (37, 38). In addition, it has been shown that reduced cellular cholesterol levels promote tau phosphorylation in cultured neurons (39) and *in vivo* (38). It is suggested that this enhanced tau phosphorylation in cholesterol-deficient neurons is mainly induced by enhanced MAPK/ERK1/2 activity, which is induced by an altered function of lipid rafts because of cholesterol deficiency in such rafts (40). Our recent study has shown that not only cholesterol deficiency but also sphingolipid deficiency promotes MAPK/ERK1/2 activity (41), indicating that an altered raft function, but not cholesterol itself, is responsible for enhanced ERK1/2 activity, leading to enhanced tau phosphorylation. With respect to the association between cholesterol deficiency and tauopathy, it is

of note that a perturbation of cholesterol metabolism and neurofibrillary tangle formation coexists in brains with Niemann–Pick type C1 (NPC1) disease (42–44). This suggests that NPC1 disease is a suitable model for investigating the mechanism by which altered cholesterol metabolism causes tauopathy (Fig. 1).

AD and NPC1 disease share a common pathway leading to tauopathy

Although there have been many different hypotheses for explaining the molecular basis of neurodegeneration in NPC1 disease, the continuous defective use of cholesterol in NPC1 neural tissues has been suggested to cause tauopathy (45, 46). Our recent studies have shown that tau in the brains of NPC1 model mice is hyperphosphorylated in a site-specific manner, which is accompanied by enhanced MAPK/ERK1/2 activity (45), and that reduced cholesterol levels in the lipid raft domain because of the lack of NPC1 activate MAPK/ERK1/2, which subsequently promotes tau phosphorylation (40). In support of this, enhanced tau phosphorylation accompanied by the focal deregulation of cdk5/p25 in the NPC1 mouse cerebrum has been reported (46). As free-cholesterol levels in NPC1-deficient cells markedly increase, these findings indicate that the state of tau phosphorylation is modulated not by total cellular cholesterol levels but by cholesterol levels in specific cellular compartments such as lipid rafts, leading to a change in intracellular signaling (Fig. 1C).

Recently, we have demonstrated that the amount of cholesterol in mitochondrial membranes is significantly elevated in NPC1 mouse brains, which reduces mitochondrial membrane potential, ATP synthase activity, and henceforth ATP levels, leading to neurodegeneration (47) (Fig. 1D). Our study also demonstrated that there is an optimal concentration of cholesterol in mitochondria, i.e. low and high cholesterol levels impair mitochondrial functions. These results suggest that in addition to enhanced tau phosphorylation, mitochondrial dysfunctions and the subsequent ATP deficiency may be responsible for neuronal impairment in NPC1 disease. As has been discussed above, it is suggested that altered cholesterol metabolism is associated with AD development. Importantly, it is now established that mitochondrial dysfunction is involved in AD development (48–50). Therefore, AD and NPC1 disease may share a common pathway involving cholesterol metabolism leading to neurodegeneration via mitochondrial dysfunction (51) (Fig. 1B).

Although many unclarified issues remain, particularly regarding various downstream events in the amyloid cascade, it is possible that cholesterol plays a key role in this cascade, modulating the processes that induce AD pathologies.

ApoE contributes to the maintenance of cholesterol homeostasis in neurons by generating and supplying HDL in an apoE-isoform-specific manner

The final question is how apoE is involved in this cascade. Our previous studies demonstrated that the apoE ability to generate HDL particles is isoform dependent; the amount of cholesterol released as HDL particles from apoE3-expressing astrocytes is ~2.5-fold greater than that from apoE4-expressing astrocytes with similar numbers of molecules of each apoE isoform (28). The apoE-isoform-dependent promotion (apoE4) or prevention (apoE3) of AD development may be explained by the apoE-isoform-dependent ability (apoE3 > apoE4) to generate HDL-like particles, which could supply cholesterol to neurons (27, 28). As it has been suggested that lipoprotein cholesterol plays a critical role in the repair of neurons including synaptogenesis (4) and neurite outgrowth (5), it is possible that when brain cholesterol homeostasis is impaired with aging by increased levels of oligomeric Aβ or oxysterols, both of which reduce cellular cholesterol level, HDL supply to neurons from glia cells of *apoE3* genotype is greater than that of *apoE4* genotype. The lower ability of apoE4 to generate and supply HDL may result in earlier disruption in cholesterol homeostasis in neurons, leading to tauopathy (Fig. 1E). The different viewpoints presented here may help in elucidating the cholesterol-dependent promotion of AD pathogenesis, in which key molecules such as Aβ and cholesterol, tauopathy, and neuronal death are significantly integrated in one schema (Fig. 1).

References

1. Roheim PS, Carey M, Forte T, Vega GL. Apolipoproteins in human cerebrospinal fluid. Proc Natl Acad Sci USA 1979;76:4646–9.
2. Pitas RE, Boyles JK, Lee SH, Hui D, Weisgraber KH. Lipoproteins and their receptors in the central nervous system. Characterization of the lipoproteins in cerebrospinal fluid and identification of apolipoprotein B,E(LDL) receptors in the brain. J Biol Chem 1987;262:14352–60.
3. Linton MF, Gish R, Hubl ST et al. Phenotypes of apolipoprotein B and apolipoprotein E after liver transplantation. J Clin Invest 1991;88:270–81.
4. Mauch DH, Nagler K, Schumacher S et al. CNS synaptogenesis promoted by glia-derived cholesterol. Science 2001;294:1354–7.

5. Hayashi H, Campenot RB, Vance DE, Vance JE. Glial lipoproteins stimulate axon growth of central nervous system neurons in compartmented cultures. J Biol Chem 2004;**279**:14009–15.
6. Saito M, Benson EP, Rosenberg A. Metabolism of cholesterol and triacylglycerol in cultured chick neuronal cells, glial cells, and fibroblasts: accumulation of esterified cholesterol in serum-free culture. J Neurosci Res 1987;**18**:319–25.
7. Ladu MJ, Gilligan SM, Lukens JR et al. Nascent astrocyte particles differ from lipoproteins in CSF. J Neurochem 1998;**70**:2070–81.
8. Craig AM, Banker G. Neuronal polarity. Annu Rev Neurosci 1994;**17**:267–310.
9. Okabe S, Kim HD, Miwa A, Kuriu T, Okado H. Continual remodeling of postsynaptic density and its regulation by synaptic activity. Nat Neurosci 1999;**2**:804–11.
10. Notkola IL, Sulkava R, Pekkanen J et al. Serum total cholesterol, apolipoprotein E epsilon 4 allele, and Alzheimer's disease. Neuroepidemiology 1998;**17**:14–20.
11. Kivipelto M, Helkala EL, Hanninen T et al. Midlife vascular risk factors and late-life mild cognitive impairment: a population-based study. Neurology 2001;**56**:1683–989.
12. Bouthillier D, Sing CF, Davignon J. Apolipoprotein E phenotyping with a single gel method: application to the study of informative matings. J Lipid Res 1983;**24**:1060–9.
13. Davignon J, Gregg RE, Sing CF. Apolipoprotein E polymorphism and atherosclerosis. Arteriosclerosis 1988;**8**:1–21.
14. Lehtinen S, Lehtimaki T, Sisto T et al. Apolipoprotein E polymorphism, serum lipids, myocardial infarction and severity of angiographically verified coronary artery disease in men and women. Atherosclerosis 1995;**114**:83–91.
15. Braeckman L, de Bacquer D, Rosseneu M, De Backer G. Apolipoprotein E polymorphism in middle-aged Belgian men: phenotype distribution and relation to serum lipids and lipoproteins. Atherosclerosis 1996;**120**:67–73.
16. Frikke-Schmidt R, Nordestgaard BG, Agerholm-Larsen B, Schnohr P, Tybjaerg-Hansen A. Context-dependent and invariant associations between lipids, lipoproteins, and apolipoproteins and apolipoprotein E genotype. J Lipid Res 2000;**41**:1812–22.
17. Wolozin B, Kellman W, Ruosseau P, Celesia GG, Siegel G. Decreased prevalence of Alzheimer disease associated with 3-hydroxy-3-methyglutaryl coenzyme A reductase inhibitors. Arch Neurol 2000;**57**:1439–43.
18. Simons M, Keller P, de Strooper B, Beyreuther K, Dotti CG, Simons K. Cholesterol depletion inhibits the generation of β-amyloid in hippocampal neurons. Proc Natl Acad Sci U S A 1998;**95**:6460–4.
19. Fassbender K, Simons M, Bergmann C et al. Simvastatin strongly reduces levels of Alzheimer's disease beta-amyloid peptides Abeta 42 and Abeta 40 *in vitro* and *in vivo*. Proc Natl Acad Sci U S A 2001;**98**:5856–61.
20. Molander-Melin M, Blennow K, Bogdanovic N, Dellheden B, Mansson JE, Fredman P. Structural membrane alterations in Alzheimer brains found to be associated with regional disease development; increased density of gangliosides GM1 and GM2 and loss of cholesterol in detergent-resistant membrane domains. J Neurochem 2005;**92**:171–82.
21. Abad-Rodriguez J, Ledesma MD, Craessaerts K et al. Neuronal membrane cholesterol loss enhances amyloid peptide generation. J Cell Biol 2004;**167**:953–60.
22. Fagan AM, Younkin LH, Morris JC et al. Differences in the A40/A42 ratio associated with cerebrospinal fluid lipoproteins as a function of apolipoprotein E genotype. Ann Neurol 2000;**48**:201–10.
23. Fassbender K, Stroick M, Bertsch T et al. Effects of statins on human cerebral cholesterol metabolism and secretion of Alzheimer amyloid peptide. Neurology 2002;**59**:1257–8.
24. Jurevics H, Hostettler J, Barrett C, Morell P, Toews AD. Diurnal and dietary-induced changes in cholesterol synthesis correlate with levels of mRNA for HMG-CoA reductase. J Lipid Res 2000;**41**:1048–54.
25. Jarvik GP, Wijsman EM, Kukull WA, Schellenberg GD, Yu C, Larson EB. Interactions of apolipoprotein E genotype, total cholesterol level, age, and sex in prediction of Alzheimer's disease: a case–control study. Neurology 1995;**45**:1092–6.
26. Evans RM, Emsley CL, Gao S et al. Serum cholesterol, APOE genotype, and the risk of Alzheimer's disease: a population-based study of African Americans. Neurology 2000;**54**:240–2.
27. Michikawa M, Fan QW, Isobe I, Yanagisawa K. Apolipoprotein E exhibits isoform-specific promotion of lipid efflux from astrocytes and neurons in culture. J Neurochem 2000;**74**:1008–16.
28. Gong JS, Kobayashi M, Hayashi H et al. Apolipoprotein E (apoE)-isoform-dependent lipid release from astrocytes prepared from human-apoE3- and apoE4-knock-in mice. J Biol Chem 2002;**277**:29919–26.
29. Hoshino T, Kamino K, Matsumoto M. Gene dose effect of the APOE-epsilon4 allele on plasma HDL cholesterol level in patients with Alzheimer's disease. Neurobiol Aging 2002;**23**:41–5.
30. Merched A, Xia Y, Visvikis S, Serot JM, Siest G. Decreased high-density lipoprotein cholesterol and serum apolipoprotein AI concentrations are highly correlated with the severity of Alzheimer's disease. Neurobiol Aging 2000;**21**:27–30.
31. Mulder M, Ravid R, Swaab DF et al. Reduced levels of cholesterol, phospholipids, and fatty acids in cerebrospinal fluid of Alzheimer disease patients are not related to apolipoprotein E4. Alzheimer Dis Assoc Disord 1998;**12**:198–203.
32. Roher AE, Weiss N, Kokjohn TA et al. Increased A beta peptides and reduced cholesterol and myelin proteins characterize white matter degeneration in Alzheimer's disease. Biochemistry 2002;**41**:11080–90.
33. Walsh DM, Klyubin I, Fadeeva JV, Rowan MJ, Selkoe DJ. Amyloid-beta oligomers: their production, toxicity and therapeutic inhibition. Biochem Soc Trans 2002;**30**:552–7.
34. Michikawa M, Gong JS, Fan QW, Sawamura N, Yanagisawa K. A novel action of Alzheimer's amyloid b-protein (Ab): oligomeric Ab promotes lipid release. J Neurosci 2001;**21**:7226–35.
35. Gong JS, Sawamura N, Zou K, Sakai J, Yanagisawa K, Michikawa M. Amyloid β-protein affects cholesterol metabolism in cultured neurons: implications for pivotal role of cholesterol in the amyloid cascade. J Neurosci Res 2002;**70**:438–46.
36. Zou K, Gong JS, Yanagisawa K, Michikawa M. A novel function of monomeric amyloid β-protein serving as an antioxidant molecule against metal-induced oxidative damage. J Neurosci 2002;**22**:4833–4841.
37. Fan QW, Yu W, Gong JS et al. Cholesterol-dependent modulation of dendrite outgrowth and microtubule stability in cultured neurons. J Neurochem 2002;**80**:178–90.
38. Koudinov AR, Koudinova NV. Essential role for cholesterol in synaptic plasticity and neuronal degeneration. Faseb J 2001;**15**:1858–60.

39. Fan QW, Wei Y, Senda T, Yanagisawa K, Michikawa M. Cholesterol-dependent modulation of tau phosphorylation in cultured neurons. J Neurochem 2001;**76**:391–400.
40. Sawamura N, Gong JS, Chang TY, Yanagisawa K, Michikawa M. Promotion of tau phosphorylation by MAP kinase Erk1/2 is accompanied by reduced cholesterol level in detergent-insoluble membrane fraction in Niemann–Pick C1-deficient cells. J Neurochem 2003;**84**:1086–96.
41. Sawamura N, Ko M, Yu W et al. Modulation of amyloid precursor protein cleavage by cellular sphingolipids. J Biol Chem 2004;**279**:11984–91.
42. Suzuki K, Parker CC, Pentchev PG et al. Neurofibrillary tangles in Niemann–Pick disease type C. Acta Neuropathol (Berl) 1995;**89**:227–38.
43. Auer IA, Schmidt ML, Lee VM et al. Paired helical filament tau (PHFtau) in Niemann–Pick type C disease is similar to PHFtau in Alzheimer's disease. Acta Neuropathol (Berl) 1995;**90**:547–51.
44. Love S, Bridges LR, Case CP. Neurofibrillary tangles in Niemann–Pick disease type C. Brain 1995;**118**(Pt 1): 119–29.
45. Sawamura N, Gong JS, Garver WS et al. Site-specific phosphorylation of tau accompanied by activation of mitogen-activated protein kinase (MAPK) in brains of Niemann–Pick type C mice. J Biol Chem 2001;**276**:10314–9.
46. Bu B, Li J, Davies P, Vincent I. Deregulation of cdk5: hyperphosphorylation, and cytoskeletal pathology in the Niemann–Pick type C murine model. J Neurosci 2002;**22**:6515–25.
47. Yu W, Gong JS, Ko M, Garver WS, Yanagisawa K, Michikawa M. Altered cholesterol metabolism in Niemann–Pick type C1 mouse brains affects mitochondrial function. J Biol Chem 2005;**280**:11731–9.
48. Hirai K, Aliev G, Nunomura A et al. Mitochondrial abnormalities in Alzheimer's disease. J Neurosci 2001;**21**:3017–23.
49. Cardoso SM, Proenca MT, Santos S, Santana I, Oliveira CR. Cytochrome C oxidase is decreased in Alzheimer's disease platelets. Neurobiol Aging 2004;**25**:105–10.
50. Abramov AY, Canevari L, Duchen MR. Beta-amyloid peptides induce mitochondrial dysfunction and oxidative stress in astrocytes and death of neurons through activation of NADPH oxidase. J Neurosci 2004;**24**:565–75.
51. Michikawa M. Cholesterol paradox: is high total or low HDL cholesterol level a risk for Alzheimer's disease? J Neurosci Res 2003;**72**:141–6.
52. Michikawa M, Yanagisawa K. Inhibition of cholesterol production but not of nonsterol isoprenoid products induces neuronal cell death. J Neurochem 1999;**72**:2278–85.

luciferase method using the ATP Bioluminescence Assay Kit CLS II (Roche) in a luminescence spectrometer.

For the determination of ATP synthase activity, 100 μg of mitochondrial protein from each sample was used to measure the synthesis of ATP. The reaction was initiated by adding 100 μg of mitochondrial protein into 100 μl of reaction buffer (10 mM K_2HPO_4, pH 7.4, 300 mM D-mannitol, 10 mM KCl, and 5 mM $MgCl_2$) at 37 °C. After a period of 1 min, 10 μl of ADP (50 μM) was added, and the intensity of bioluminescene was recorded at 37 °C, where the peak height was proportional to the amount of ATP that was synthesized.

Effect of Removal of Cholesterol from the Mitochondria Membrane—To remove cholesterol from the mitochondria membrane, a stock solution of methyl-β-cyclodextrin (Sigma) (150 mM) was prepared using distilled water, and then diluted into the P2 fraction derived from brains to a final concentration of 7.5 mM. The mixture was incubated for 20 min at 37 °C, followed by an additional incubation for 10 min at room temperature and subjected to ultracentrifugation to purify mitochondria. For the cholesterol enrichment of mitochondria with or without methyl-β-cyclodextrin, a stock solution of cholesterol was prepared (5 mM in 100% ethanol) and added into the P2 fraction that was resuspended in isolation buffer (200 μl) at a final concentration of 50 μM, followed by incubation for 20 min at 37 °C. The mitochondria were rinsed twice and subjected to ultracentrifugation to purify mitochondria. The cholesterol level, protein content, and the ATP synthase activity associated with mitochondria were then determined as described above.

Immunoblot Analysis—Immunoblot analysis was performed as previously described (5). The primary antibodies used were mouse monoclonal antibodies (cytochrome *c*, 1:1,000 dilution; Na^+,K^+-ATPase β2, 1:1000 dilution; GM130, 1:500 dilution; Bip/GRP78, 1:500 dilution; cathepsin L, 1:1000 dilution; nucleoporin p62, 1:1000 dilution; and cytochrome *c* oxidase subunit I, 1:1000 dilution), and rabbit polyclonal antibodies (VDAC, 1:1000 dilution; fumarase, 1:500 dilution; and UCP-2, 1:1,000 dilution). After rinsing and incubation in the presence of appropriate peroxidase-conjugated secondary antibody, the respective bands were detected with an ECL kit (Amersham Biosciences).

Morphological Analysis—Cultured neurons maintained for 1, 2, and 3 days in serum-free medium in the presence or absence of 0.5 mM ATP, 0.5 mM ADP, or 0.5 mM AMP-PNP (Roche) were rinsed and then fixed for 20 min at room temperature in 0.1 M PBS containing 4% paraformaldehyde fluoride. The cells were then rinsed with PBS, blocked in PBS containing 2.0% BSA, then incubated with monoclonal anti-β-tubulin antibody (Covance, Richmond, CA, 1:500 dilution) in PBS containing 2% BSA overnight at 4 °C. The cells were then incubated with anti-mouse IgG (1:200) in 0.1 M PBS, 0.5% BSA for 1 h, rinsed, and visualized using the ABC method. Photographic images were captured using a CCD camera (DC500) (Leica Microsystems GMBH, Wetzar, Germany) attached with phase-contrast microscopy (Olympus IX70, Olympus Co. Ltd., Tokyo, Japan). The ratio of neurite number/cell and neurite total length/cell was determined using an image analyzer (LSM 510, Carl Zeiss Co., Ltd., Jena, Germany).

Determination of Cholesterol and Phosphatidylcholine (PC) Transport—To determine the transport of exogenously added cholesterol and PC into mitochondria in cultured cells, wild type astrocytes were labeled with 37 Bq/ml of [^{14}C]acetate (PerkinElmer Life Sciences). The conditioned media was collected 5 days later and an equivalent amount of ^{14}C-labeled HDL (cholesterol concentration at 1 μg/ml) was added into plates previously seeded with NPC1+/+, NPC1+/−, and NPC1−/− astrocytes. The cells were harvested at 4, 8, and 12 h following the addition of HDL and the mitochondria were isolated. The lipids were separated using sequential one-dimensional chromatography and the amounts of [^{14}C]cholesterol and [^{14}C]PC were quantified using BAS2500 (Fuji Film, Tokyo, Japan) as previously described (24).

To measure lipid efflux from mitochondria and cells, cultured astrocytes were labeled for 5 days with ^{14}C-labeled HDL. Five days following the commencement of labeling, the cells were rinsed in DMEM three times and incubated in DMEM. The cells were then harvested at 0, 2, and 4 h, and mitochondria were isolated from each culture. The amounts of [^{14}C]cholesterol and [^{14}C]PC remaining in the mitochondria and cells were determined as described above.

Lipid Analysis—The concentration of cholesterol was determined using a cholesterol determination kit, LTCII (Kyowa Medex, Tokyo), whereas the concentration of phospholipids was determined using a phospholipid determination kit, PLB (Wako, Osaka, Japan), as previously described (24).

Statistical Analysis—Statistical analysis was performed using StatView computer software, and multiple pairwise comparisons among groups of data were performed using the analysis of variance, and the Bonferroni *t* test.

RESULTS

The Morphology and Membrane Potential of Mitochondria in Neurons and Astrocytes Isolated from Mouse Brains—The morphology and function of mitochondria were examined in NPC1+/+, NPC1+/−, and NPC1−/− mouse brains, and cultured cells prepared from cerebral cortices using electron and confocal microscopy. The examination of NPC1+/+ and NPC1−/− mouse brains using electron microscopy revealed that NPC1−/− mouse brains contained smaller and more rounded mitochondria, with a translucent matrix and irregular cisternae (Fig. 1, *a* and *b*). Next, the membrane potential of mitochondrial membrane within cultured neurons and astrocytes was determined using Mitotracker JC-1 (30). When mitochondrial membrane potential is normally polarized, JC-1 concentrates in the mitochondria and aggregates, resulting in a high red/green fluorescence intensity ratio. However, with decreasing mitochondrial membrane potential, there is less aggregation of Mitotracker JC-1, therefore resulting in decreased red/green fluorescence intensity ratio. The results indicated a marked decrease in red fluorescence intensity in NPC1−/− neurons (Fig. 1*e*) compared with NPC1+/+ (Fig. 1*c*) and NPC1+/− neurons (Fig. 1*d*). In contrast, there was a marked increase in green fluorescence intensity observed in NPC1−/− neurons (Fig. 1*h*), compared with NPC1+/+ neurons (Fig. 1*f*) and NPC1+/− neurons (Fig. 1*g*). Similarly, there was a marked decrease in red fluorescence intensity in NPC1−/− astrocytes (Fig. 1*n*) compared with NPC1+/+ neurons (Fig. 1*l*) and NPC1+/− astrocytes (Fig. 1*m*) and a marked increase in green fluorescence intensity in NPC1−/− astrocytes (Fig. 1*q*) compared with NPC1+/+ astrocytes (Fig. 1*o*) and NPC1+/− astrocytes (Fig. 1*p*). However, this being the case, there was no significant difference noticed in the survival of NPC1+/+, NPC1+/−, and NPC1−/− neurons and astrocytes (data not shown). Together, these results indicate that NPC1−/− neurons and astrocytes have an altered structure and altered membrane potential of mitochondria.

The Level of ATP in Brain, Muscle, Liver, and Cultured Cortical Neurons—The level of ATP was determined in brain, muscle, and liver from NPC1+/+, NPC1+/−, and NPC1−/− mice at 9 weeks of age. The results indicate that the level of ATP in these tissues derived from NPC1−/− mice are significantly decreased compared with that derived from NPC1+/+ and NPC1+/− mice (Fig. 2*a*). As an internal control for the amount of mitochondria used in each sample, immunoblot analysis was performed to determine the amount of VDAC, a protein that resides in the outer membrane of mitochondria (Fig. 2, *insets*). The addition of ATP into the liver samples (20 nmol of ATP/mg of protein) resulted in increased levels of ATP by ~15 nmol/mg of protein in the three genotypes, excluding a possibility that the ATP degradation rate is accelerated in NPC1−/− tissues. The level of ATP was also determined in cultured cortical neurons prepared from NPC1+/+, NPC1+/−, and NPC1−/− mice at embryonic day 16, and maintained and harvested at days 3 and 6 of culture (Fig. 2*b*). The results again indicate that the level of ATP in neurons prepared from NPC1−/− mouse brains are significantly decreased compared with neurons prepared from NPC1+/+ and NPC1+/− mouse brains.

Enzymatic Analysis of Mitochondria Complexes I + III, II + III, IV, and V Using Purified Mitochondria from Mouse Brains—To determine which step(s) in ATP metabolism might be affected in NPC1−/− cells, the activities of respiratory complex I + III (NADH-cytochrome *c* oxidoreductase), complex II + III (succinate-cytochrome *c* oxidoreductase), complex IV (cytochrome *c* oxidase), and ATP synthase (complex V) were deter-

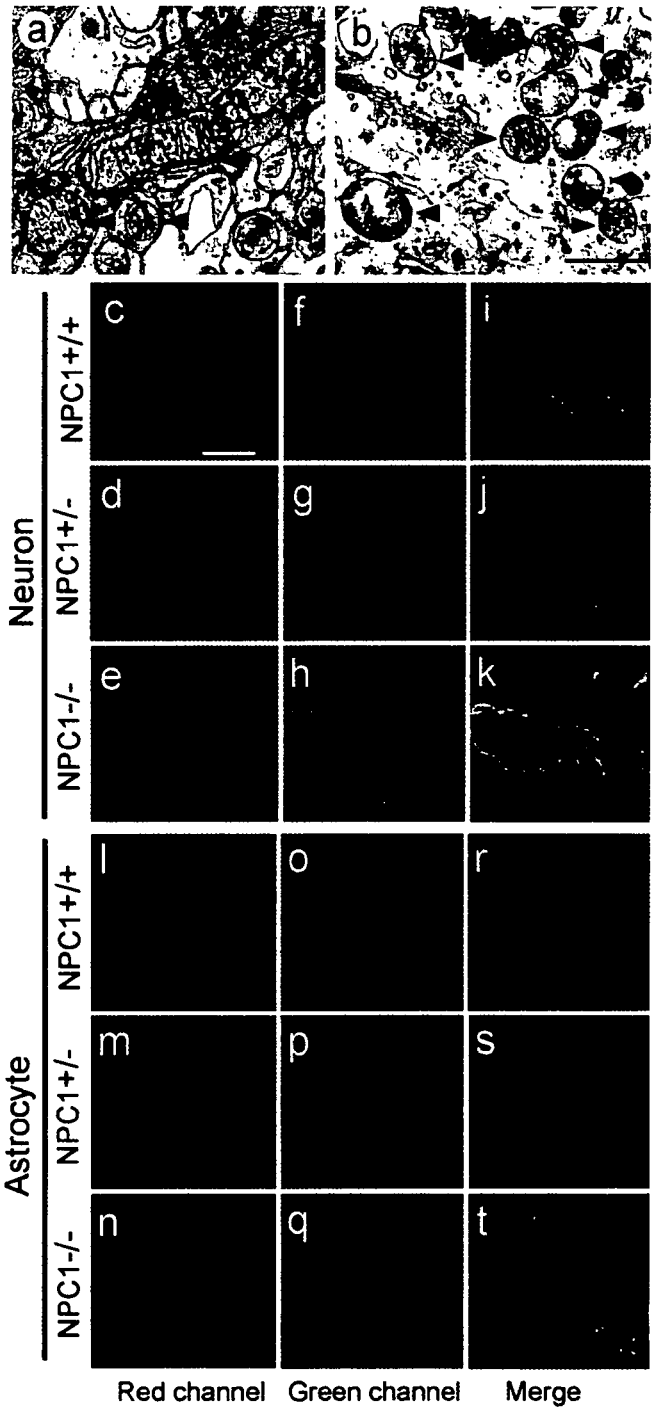

FIG. 1. **The morphology and membrane potential of mitochondria in neurons and astrocytes isolated from mouse brains.** Electron microscopy was performed on brains from NPC1+/+ (*a*) and NPC1−/− (*b*) mice at 9 weeks of age. *Arrowheads* indicate the mitochondria. *Bar* = 1 μm. The mitochondrial membrane potential for cultured neurons (*c–k*) and astrocytes (*l–t*) prepared from NPC1+/+, NPC1+/−, and NPC1−/− mouse brains was determined by staining with Mitotracker JC-1. Cells stained with JC-1 were viewed by confocal microscopy using the red channel for neurons (*c*, *d*, and *e*) and astrocytes (*l*, *m*, and *n*), whereas the green channel was used for neurons (*f*, *g*, and *h*) and astrocytes (*o*, *p*, and *q*). The merge images for neurons (*i*, *j*, and *k*) and astrocytes (*r*, *s*, and *t*) are also shown. *Bar* = 25 μm.

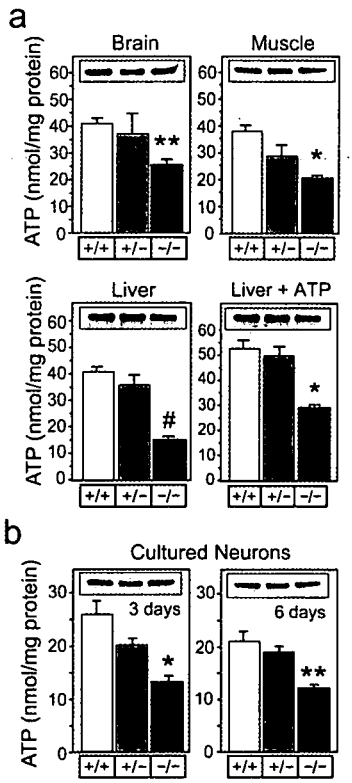

FIG. 2. **The level of ATP in mouse brain, muscle, liver, and cultured neurons.** The level of ATP was determined in brain, muscle, and liver removed from NPC1+/+, NPC1+/−, and NPC1−/− mice at 9 weeks of age (*a*). In addition, the level of ATP was also determined in liver samples for which ATP was added at a concentration of 20 nmol/mg of protein. For each of the samples, an equivalent amount of protein was used to compare the level of ATP. *, $p < 0.002$ and 0.05 *versus* NPC1+/+ and NPC1+/−, respectively. **, $p < 0.03$ *versus* NPC1+/+ and NPC1+/−. #, $p < 0.001$ *versus* NPC1+/+ and NPC1+/−. Data show mean ± S.E. of four samples. Three independent experiments show similar results. *b*, the level of ATP was determined in cultured cortical neurons prepared from NPC1+/+, NPC1+/−, and NPC1−/− mouse brains on embryonic day 16. For each of the samples, an equivalent amount of protein isolated from neurons maintained in serum-free media and harvested at days 3 and 6 in culture were used to compare the level of ATP. *, $p < 0.002$ *versus* NPC1+/+ and *, $p < 0.05$ *versus* NPC1+/−. **, $p < 0.03$ *versus* NPC1+/+ and NPC1+/−. For each of the respective tissues and cultured cortical neurons, immunoblot analysis of VDAC was used as an internal control (*a* and *b*, *inset*). The results represent the mean ± S.E. of four different samples, and are representative of three independent experiments.

mined in purified mitochondrial fractions isolated from NPC1+/+, NPC1+/−, and NPC1−/− mouse brains at 9 weeks of age. The purity of mitochondria in the P3 fraction isolated from a NPC1+/+ mouse brain was confirmed by enrichment of cytochrome *c* oxidase, and the absence of specific markers, such as lysosomal (cathepsin L), endoplasmic reticulum (Bip/GRP78), Golgi apparatus (GM130), and plasma membrane (Na^+,K^+-ATPase) markers (Fig. 3*a*). Furthermore, the purity of mitochondria in the P3 fraction isolated from a NPC1+/+ mouse brain was confirmed by electron microscopy (Fig. 3*b*). The results indicated there were no significant differences in the enzyme activities associated with complexes I + III, II + III, and IV of the different mouse brains that were analyzed (Fig. 3*c*). In contrast, the enzyme activities associated with complex V for the hydrolysis of ATP (F_1F_0-ATPase), and for the synthesis of ATP (ATP synthase), were significantly decreased in mitochondria isolated from NPC1−/− brains, compared with those from NPC1+/+ and NPC1+/− (Fig. 3*d*). These results are consistent with and explain the observation that total ATP levels are decreased in NPC1−/− tissues (Fig. 2*a*) and neurons (Fig. 2*b*). Because the synthesis of ATP is not entirely regulated by the coupling of sequential oxidation steps through the respiratory chain, but also by the mitochondrial uncoupling proteins (UCPs) (31), we also examined the amount of UCP-2 residing in the mitochondria fraction isolated from mouse brain using immunoblot analysis. The amount of UCP-2 determined

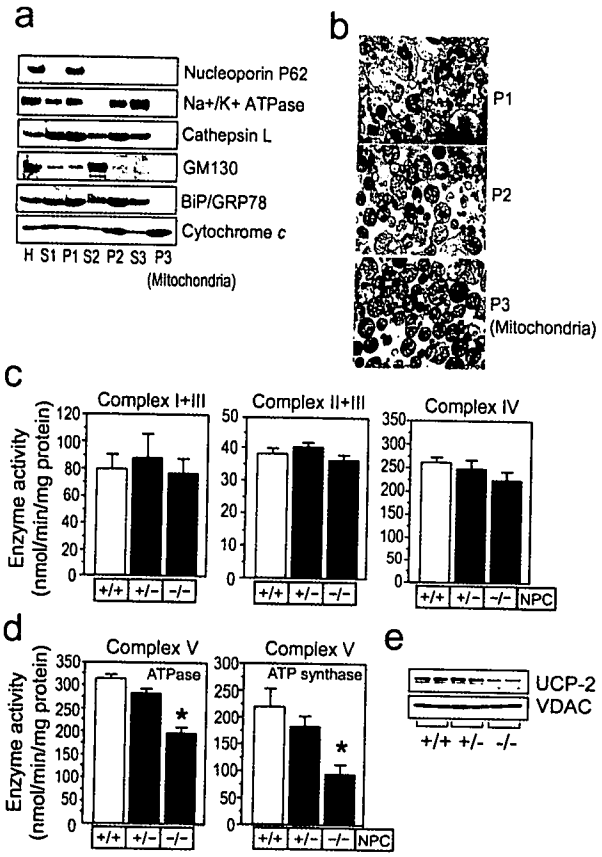

FIG. 3. **Enzymatic analysis of mitochondria complexes I + III, II + III, IV, and V using purified mitochondria from mouse brains.** The enzyme activity of mitochondria complexes I + III, II + III, IV, and V were determined in brains from NPC1+/+, NPC1+/−, and NPC1−/− mice at 9 weeks of age. The fraction containing purified brain mitochondria (*P3*), along with other cellular fractions (*P1*, *P2*, *P3*, *S1*, and *S2*), were isolated as described under "Experimental Procedures." The purity of mitochondria was confirmed by determining the distribution of specific markers such as cytochrome *c* oxidase (mitochondria), cathepsin L (lysosomal), Bip/GRP78 (endoplasmic reticulum), GM130 (Golgi apparatus), and Na^+,K^+-ATPase (plasma membrane) using immunoblot analysis (*a*). Electron microscopy (EM) analysis of P1, P2, and P3 fractions, isolated from a NPC1+/+ mouse brain was performed to demonstrate purification of mitochondria in the P3 fraction (*b*). The enzymatic analysis of complexes I + III, II + III, and IV was determined using P3 fractions isolated from brains of NPC1+/+, NPC1+/−, and NPC1−/− mice (*c*). The enzymatic analysis of complex V was determined by measuring the hydrolysis rate of ATP (ATPase), and the synthesis rate of ATP from ADP (ATP synthesis), using P3 fractions isolated from brains of NPC1+/+, NPC1+/−, and NPC1−/− mice (*d*). *, $p < 0.01$ *versus* NPC1+/+ and NPC1+/−. The results represent the mean ± S.E. of four different samples and are representative of three independent experiments. Immunoblot analysis of each representative tissue was performed using UCP-2 and immunoblot analysis of VDAC was used as an internal control (*e*).

in mitochondria isolated from the NPC1−/− brains was markedly reduced compared with that in the mitochondria from the NPC1+/− and NPC1−/− brains (Fig. 3*e*). As an internal control, immunoblot analysis was performed to determine the amount of VDAC. These results suggest that the enhanced uncoupling respiratory chain function from ATP synthesis by UCP-2 is not involved in the decreased ATP synthesis in NPC1−/− tissues, and that the expression of UCP-2 is downregulated possibly because of a negative feedback regulation.

Because there may be a possibility that the decreased levels of ATP and ATP synthase activity are because of indirect consequences caused by neuronal death occurring at 9 weeks of age, we analyzed those parameters in younger mice at 10 days of age. Similar to the results shown in Figs. 2 and 3, the levels of ATP and ATP synthase activity in NPC1−/− brains were

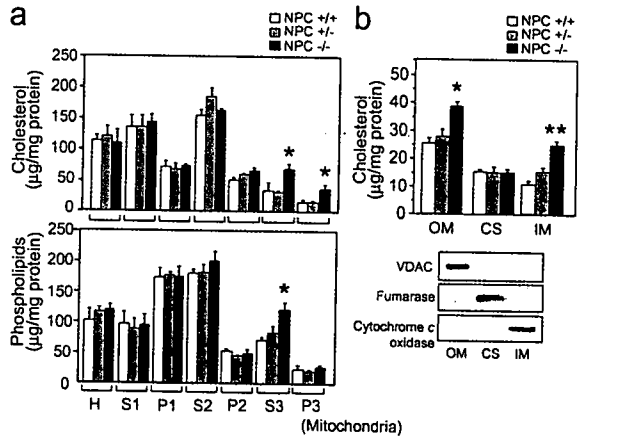

FIG. 4. **The level of cholesterol and phospholipids in cellular fractions and purified mitochondria.** The level of cholesterol and phospholipids in cellular fractions and purified mitochondria was determined in NPC1+/+, NPC1+/−, and NPC1−/− mouse brains (*a*). The level of cholesterol in the OM, CS, and the IM was determined for purified mitochondria (*P3*). The distribution of specific markers for OM (*VDAC*), CS (*fumarase*), and IM (*cytochrome c oxidase*) was determined using immunoblot analysis, and used to verify purification of the respective mitochondria membranes (*b*). *, $p < 0.0001$ and **, $p < 0.005$ *versus* NPC1+/+ and NPC1+/−. The results represent the mean ± S.E. of four different samples and are representative of three independent experiments.

significantly decreased compared with those in NPC1+/+ brains, and the cholesterol level was increased in the mitochondria that were isolated from brains of NPC1−/− mice (see Supplemental Materials, Fig. S1).

The Level of Cholesterol and Phospholipids in Cellular Fractions and Purified Mitochondria—Because the most prominent feature of NPC1−/− cells is altered cholesterol metabolism, the concentration of cholesterol and phospholipids in cellular fractions and purified mitochondria fraction (P3) was determined in NPC1+/+, NPC1+/−, and NPC1−/− mouse brains. The results indicated that the concentration of cholesterol was significantly increased in fractions S3 (enriched with plasma membrane, lysosome, and endoplasmic reticulum), and P3 (mitochondria), whereas the concentration of phospholipids was increased only in fraction S3 (Fig. 4*a*). This result would therefore exclude the possibility that contamination of lipid between fractions S3 and P3 had occurred. In addition, the concentration of cholesterol was determined for specific membranes purified from mitochondria, specifically the OM, CS, and IM. The results indicated that the concentration of cholesterol was significantly increased in both the OM and IM of mitochondria isolated from NPC1−/− mouse brains, compared with the same membranes of mitochondria isolated from NPC1+/+ and NPC1+/− mouse brains (Fig. 4*b*, *upper panel*). The purity of specific membranes purified from mitochondria was examined and confirmed using immunoblot analysis for proteins associated with the OM (VDAC), CS (fumarase, a matrix marker), and IM (cytochrome *c* oxidase) (Fig. 4*b*, *lower panel*).

Kinetic Analysis of Cholesterol and PC Transport to and from Mitochondria—Kinetic analysis of cholesterol transport to mitochondria, which was exogenously added as [^{14}C]cholesterol-labeled HDL or endogenously synthesized [^{14}C]cholesterol, was determined using astrocytes prepared from NPC1+/+, NPC1+/−, and NPC1−/− mouse brains. As indicated in Fig. 5*a*, [^{14}C]cholesterol-labeled HDL added to cells was transported into the cell homogenate and mitochondria at a higher rate in NPC1−/− cells than NPC1+/+ and NPC1+/− cells at 12 h. Similarly, the amount of [^{14}C]PC transported into NPC1−/− cells (homogenate) was at a higher rate than NPC1+/+ and NPC1+/− cells at 8 and 12 h (Fig. 5*b*). However,

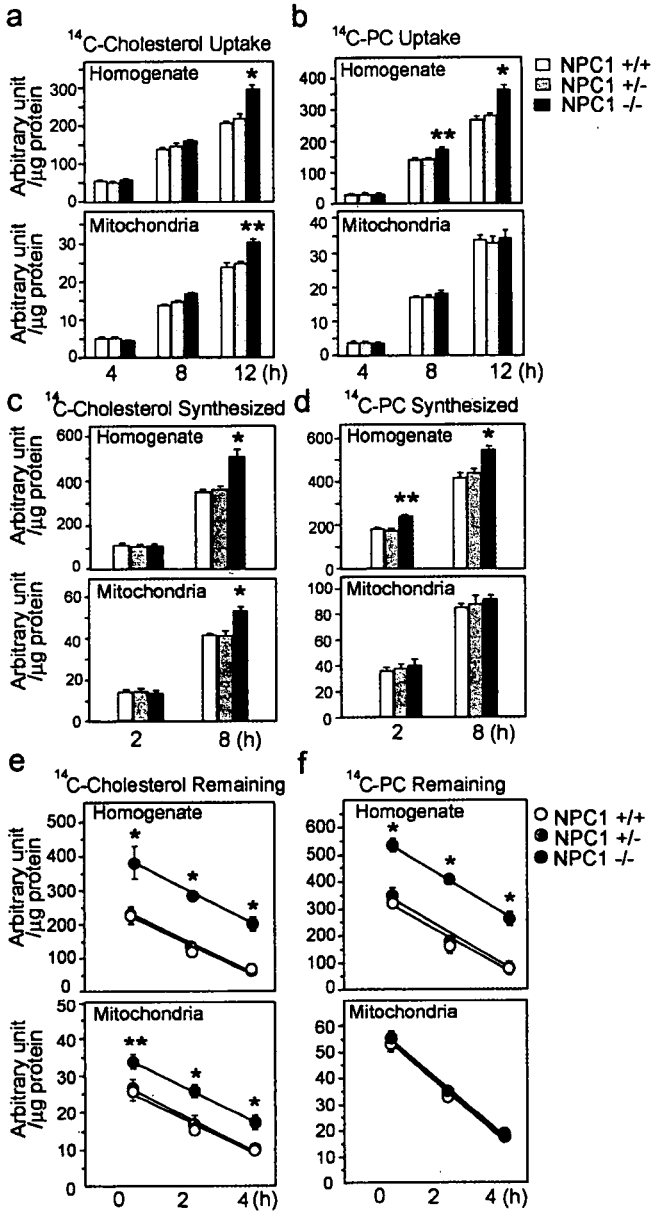

FIG. 5. **Kinetic analysis of cholesterol and PC transport to and from mitochondria.** Kinetic analysis of cholesterol and PC transport to and from mitochondria was performed using astrocytes isolated from NPC1+/+, NPC1+/−, and NPC1−/− mice. The astrocytes prepared from the brains of wild type mice were labeled with [^{14}C]acetate, and HDL containing [^{14}C]cholesterol and [^{14}C]PC was isolated as described under "Experimental Procedures." The astrocytes prepared from the brains of NPC1+/+, NPC1+/−, and NPC1−/− mice were incubated with an equivalent amount of HDL (1 μg of cholesterol/ml), and the amount of [^{14}C]cholesterol (*a*) and [^{14}C]PC (*b*) transported into the cells and mitochondria were determined. *, $p < 0.001$ and **, $p < 0.05$ *versus* NPC1+/+ and NPC1+/−. The amount of endogenously synthesized cholesterol (*c*) and PC (*d*) in the cell homogenate and transported to mitochondria was determined. *, $p < 0.001$ and **, $p < 0.01$ *versus* NPC1+/+ and NPC1+/−. The amount of lipid removed from astrocytes, and mitochondria isolated from astrocytes, was determined using astrocytes cultures prepared from NPC1+/+, NPC1+/−, and NPC1−/− mouse brains as described under "Experimental Procedures." The levels of [^{14}C]cholesterol (*e*) and [^{14}C]PC (*f*) remaining in the cells and mitochondria were determined after 0, 2, and 4 h of incubation with labeled HDL. *, $p < 0.0001$ and **, $p < 0.002$ *versus* NPC1+/+ and NPC1+/−. For studies *a–f*, the results indicate the mean ± S.E. of four samples, and are representative of two independent experiments.

there was no significant difference in the transport of exogenously added PC into mitochondria among the three genotypes (Fig. 5*b*, *lower panel*). The level of endogenously synthesized cholesterol and PC in the homogenate and that transported into mitochondria were also determined. The results indicated that there was a higher rate of synthesis of cholesterol and PC in NPC1−/− cells (homogenate) compared with NPC1+/+ and NPC1+/− cells (Fig. 5, *c* and *d*). However, although the transport of endogenously synthesized cholesterol into mitochondria of NPC1−/− cells was higher than NPC1+/+ and NPC1+/− cells, there was no significant difference in the transport of endogenously synthesized PC into mitochondria among the three genotypes (Fig. 5, *c* and *d*, *lower panels*).

Next, the kinetics of cholesterol and PC removal from cells and mitochondria were determined. The results indicated that the amount of [^{14}C]cholesterol remaining in the cell homogenate and mitochondria decreased with time, however, the amount of [^{14}C]cholesterol in the cell homogenate and mitochondria of NPC1−/− cells was significantly higher compared with NPC1+/+ and NPC1+/− cells at every time point examined (Fig. 5*e*). In contrast, there was no difference in the level of remaining [^{14}C]PC in mitochondria among the three genotypes (Fig. 5*f*, *lower panel*). The rates of cholesterol removal calculated from the data shown in Fig. 5*e* are 40.5, 42.5, and 42.8 (arbitrary unit/h/μg of protein) from cells (homogenate), and 4.0, 4.1, and 4.3 (arbitrary unit/h/μg of protein) from mitochondria of NPC1+/+, NPC1+/−, and NPC1−/− cells, respectively, indicating that the rate of cholesterol removal is not adversely affected in NPC1−/− cells.

An Increase in the Level of Mitochondria Membrane Cholesterol Inhibits ATP Synthase—To determine whether an increase in mitochondrial cholesterol adversely affects mitochondria function, the activity of ATP synthase was determined in relation to the amount of cholesterol associated with mitochondria isolated from NPC1+/+ and NPC1−/− mouse brains. To perform this study, the hydrophilic cholesterol-sequestering agent, methyl-β-cyclodextrin, was used to remove cholesterol from mitochondria membranes. After incubation of mitochondria with 7.5 mM methyl-β-cyclodextrin, results indicated that the level of cholesterol associated with NPC1−/− mitochondria, which was significantly increased compared with NPC1+/+ mitochondria, was reduced to a level similar to that of NPC1+/+ mitochondria (Fig. 6*b*). In accordance with this decrease in the level of cholesterol associated with NPC1−/− mitochondria, the activity of ATP synthase was significantly increased to a level similar to that of NPC1+/+ mitochondria (Fig. 6*a*). Importantly, when the decreased cholesterol level in NPC1−/− mitochondria induced by incubation with methyl-β-cyclodextrin was recovered by the subsequent incubation with 50 μM cholesterol (Fig. 6*b*, *right panel*), the enhanced ATP synthase activity induced by methyl-β-cyclodextrin was reduced to a level similar to that of nontreated NPC1−/− mitochondria (Fig. 6*a*, *right panel*). In addition, the results using NPC1+/+ mitochondria indicate that when the cholesterol level in the mitochondria was increased or decreased, the activity of ATP synthase was reduced in either case (Fig. 6, *a* and *b*, *left panels*), suggesting that there is an optimal level of cholesterol in the mitochondrial membrane for ATP synthase.

Impaired Neuronal Outgrowth in NPC1−/− Neurons Is Restored by ATP Treatment in Culture—Because ATP is required for the development of neurons (32), the effect of NPC1 deficiency on neurite outgrowth was investigated using neurons prepared from cerebral cortices derived from NPC1+/+, NPC1+/−, and NPC1−/− mouse brains. Using immunocytochemistry, the staining neurons for β-tubulin indicated that while neurite extension was clearly evident at 72 h in NPC1+/+ and NPC1+/− neurons, it was impaired in NPC1−/− neurons (Fig. 7*A*, *a*, *c*, and *e*). In addition, the time-dependent analysis of neurite outgrowth indicated that neurite

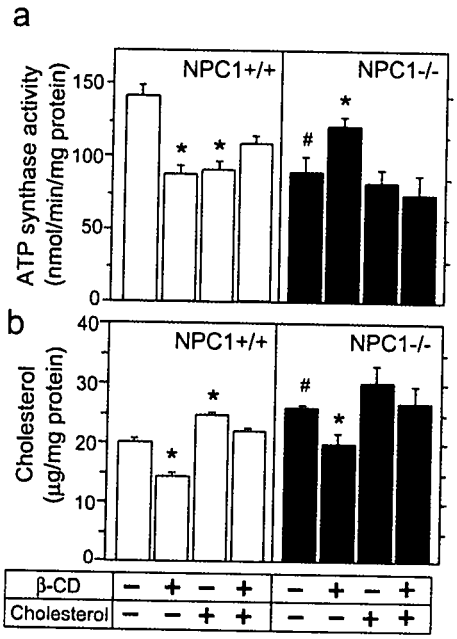

FIG. 6. **Modulation of ATP synthase activity by cholesterol in the mitochondrial membrane.** The activity of ATP synthase was determined in relation to the level of cholesterol associated with mitochondria isolated from NPC1+/+ and NPC1−/− mouse brains. The brain P2 fractions isolated from another these mouse brains was incubated in the presence of methyl-β-cyclodextrin (β-CD) (7.5 mM) or cholesterol (50 μM) for 20 min at 37 °C, followed by centrifugation to isolate mitochondria (P3). For β-CD and cholesterol treatment, the P2 fraction was incubated with β-CD, rinsed, and then incubated with cholesterol for 20 min at 37 °C, followed by centrifugation to isolate mitochondria. The activity of ATP synthase per mitochondrial protein (*top panel*) and the concentration of cholesterol (*bottom panel*) associated with the purified mitochondria were determined as described under "Experimental Procedures." *, $p < 0.02$ *versus* control (nontreatment); #, $p < 0.01$ *versus* NPC1+/+ control. The results represent the mean ± S.E. of three different samples and are representative of three independent experiments.

extension and sprouting were significantly suppressed in NPC1−/− neurons, compared with NPC1+/+ and NPC1+/− neurons (Fig. 7*B*, *a* and *c*). Importantly, both the neurite length and number were restored upon addition of 0.5 mM ATP (Fig. 7, *A*, *f*, and *B*, *b* and *d*). We have confirmed that ATP added extracellularly remains in the medium and increased cellular ATP levels for at least 24 h (see Supplemental Materials, Fig. S2). Next, the effect of nucleotides other than ATP, such as ADP and AMP-PNP, on neurite outgrowth was determined. The results indicated that ADP added extracellularly had no significant effect on neurite outgrowth (number and length) in both NPC1+/+ and NPC1−/− neurons (Fig. 7*C*, *c* and *d*). In contrast, as has been reported previously (33), the nonhydrolyzable analogue, AMP-PNP, inhibited neurite outgrowth in NPC1+/+ neurons (Fig. 7*C*, *c* and *d*). The levels of ATP in cultured neurons in the absence or presence of ATP, ADP, or AMP-PNP were determined. Only the addition of ATP increased the cellular level of ATP (Fig. 7*C*, *a*). These results indicate that deterioration of neurite outgrowth, which is present in NPC1−/− neurons, results from a decreased level of ATP.

DISCUSSION

The molecular mechanism responsible for neurodegeneration in NPC1 disease remains undetermined. The present study describes severe mitochondrial abnormalities that may be responsible for causing impaired neuronal function and neurodegeneration in NPC1−/− mouse brains. The results from this study strongly suggest that neuronal dysfunctions and degeneration in NPC1−/− mouse brains arise from (i) a decrease in mitochondrial membrane potential, (ii) a decrease in ATP synthesis, and (iii) a decrease in the level of cellular ATP. In addition, NPC1−/− neurons exhibited impaired neurite outgrowth, which was restored by the addition of ATP to the culture media. Each of the abnormalities identified in mitochondria of NPC1−/− neurons was associated with an elevation in the cholesterol concentration of mitochondria membranes, and that by reducing the cholesterol concentration of mitochondria membranes, ATP synthase activity was restored to normal.

The results demonstrated that an increase in the level of mitochondria membrane cholesterol impaired mitochondrial function. Additional support for cholesterol being the offending metabolite was confirmed by incubating the water-soluble cholesterol sequestering agent, methyl-β-cyclodextrin, in the presence of NPC1−/− mitochondria membranes to reduce membrane cholesterol. This reduced NPC1−/− mitochondria membrane cholesterol to a level that was similar to NPC1+/+ mitochondria membranes, and enhanced ATP synthase activity. In addition, the recovering cholesterol level in the methyl-β-cyclodextrin-treated mitochondria by subsequent incubation with cholesterol decreased ATP synthase activity to an initial level. The increased molar ratio of cholesterol to phospholipids measured in NPC1−/− mitochondria membranes suggests that the basic structure and/or physical property of the mitochondria membrane is adversely affected, and that the altered physical properties of these membranes leads to a reduced proton motive force and membrane potential, which in turn decreases ATP synthesis. In support of this result, previous studies have demonstrated that an elevation of cholesterol concentration in the inner mitochondrial membrane reduces mitochondrial membrane potential, induces mitochondria depolarization and uncoupling responsible for oxidative phosphorylation, and henceforth impairing ATP synthesis (34–36). Each of these defects was also observed in NPC1−/− brains and neurons. As a result, it is possible that an increased level of cholesterol within mitochondria membranes, known to adversely influence membrane fluidity (36), leads to impaired mitochondria permeability transition, mitochondrial membrane potential, and ATP synthesis in NPC1−/− cells. Interestingly, the fact that methyl-β-cyclodextrin treatment also reduced ATP synthesis in NPC1+/+ mitochondria membranes suggests that there is an optimal ratio of cholesterol to phospholipids in mitochondria membranes for ATP synthesis.

Although the NPC1 protein has been shown to facilitate the transport of cholesterol from late endosomes/lysosomes to the trans-Golgi network, the plasma membrane, and the endoplasmic reticulum, the results of this study show that exogenously added cholesterol and endogenously synthesized cholesterol are transported into mitochondria in NPC1-deficient astrocytes. These results suggest the existence of a cholesterol transport pathway independent of the NPC1 protein. The results also suggest that while the cholesterol level in mitochondrial membranes is elevated in NPC1−/− neurons, the phospholipid level in these mitochondria membranes is similar to NPC1+/+ neurons. Finally, because the mitochondria were shown not to be contaminated by late endosomes/lysosomes using both immunoblot analysis and electron microscopy, these results suggest that cholesterol metabolism with respect to the mitochondria may be independently affected in NPC1−/− cells. It is unclear why the level of cholesterol in mitochondrial membranes increases in NPC1−/− brains, although accumulation of cholesterol in late endosome/lysosome and the increased level of *de novo* synthesis of cholesterol in NPC1−/− cells may somehow contribute to increased cholesterol transport to the mitochondrial membranes.

The similar cholesterol removal rate from mitochondria in

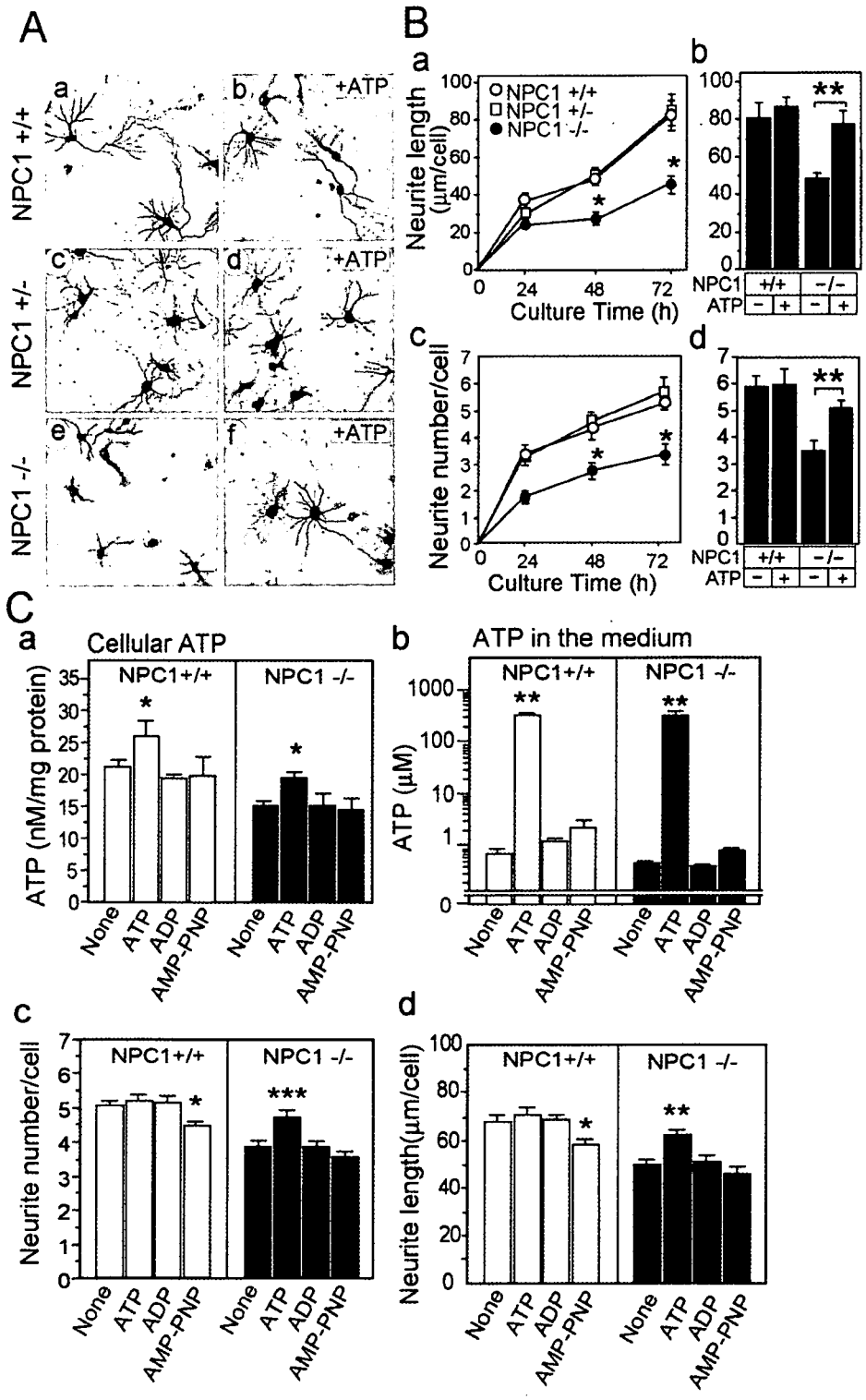

FIG. 7. **Effect of NPC1 deficiency on neurite outgrowth.** The effect of NPC1 deficiency on neurite outgrowth was investigated using neurons prepared from cerebral cortices derived from NPC1+/+, NPC1+/−, and NPC1−/− mouse brains. *A*, neurons prepared from cerebral cortices of NPC1+/+ (*a* and *b*), NPC1+/− (*c* and *d*), and NPC1−/− (*e* and *f*) were cultured in serum-free medium for 72 h, then fixed and stained for β-tubulin. *B*, neurite length/cell (*a*) and neurite number/cell (*c*) were determined as a function of time as described under "Experimental Procedures." The effect of incubating neurons in media supplemented with 0.5 mM ATP for 72 h and measuring neurite extension (*b*) and sprouting (*d*) was determined. *, $p < 0.005$ *versus* NPC1+/+ and NPC1+/− and **, $p < 0.02$. *C*, neurons prepared from cerebral cortices of NPC1+/+ and NPC1−/− mouse brains were incubated with none, ATP (0.5 mM), ADP (0.5 mM), or AMP-PNP (0.5 mM) in serum-free medium for 72 h. The cultures and the media were then harvested and the levels of cellular ATP (*a*), ATP remaining in the media (*b*), neurite length/cell (*c*), and neurite number/cell (*d*) of each treatment were determined. *, $p < 0.05$, **, $p < 0.001$, and ***, $p < 0.02$ *versus* others. These data represent the mean ± S.E. of 80 cells from each genotype and are representative of three independent experiments.

NPC1+/+, NPC1+/−, and NPC1−/− cells suggested that the elevated cholesterol level in NPC1−/− mitochondria may be because of increased cholesterol transport to mitochondria. Several mechanisms have been proposed for phospholipid transport between the mitochondria and other biological membranes (37, 38). However, cholesterol transport to and from the

mitochondria is largely unknown. The results of this study suggest that NPC1 may also modulate cholesterol transport to mitochondria, in addition to the role of NPC1 in cholesterol transport to the trans-Golgi network, the plasma membrane, and the endoplasmic reticulum (39). Unlike these cellular compartments that become relatively cholesterol-deficient when NPC1 is defective (positive regulation), mitochondria become relatively cholesterol-enriched (negative regulation). Such a mechanism proposed for the function of NPC1 would be consistent with cholesterol serving as the offending metabolite, as it adversely affects critical functions required for mitochondria.

Importantly, it is well established that mitochondria contribute to steroidogenesis. The late-limiting step in steroidogenesis involves the conversion of cholesterol into pregnenolone by cytochrome $P450_{scc}$ and its associated electron-transport chain, which are known to be associated with the inner membrane of mitochondria (40). In an elegant study recently performed by Griffin *et al.* (22) it was determined that decreased levels of neurosteroids may actually be the cause of neurodegeneration in NPC1−/− mice. However, it must be emphasized that the mechanism responsible for the loss in neurosteroids and neurosteroidogenic activity remains undefined. Because mitochondria obviously have a critical role in steroidogenesis, the altered function of mitochondria described in the present study is consistent with this organelle having a key role in promoting neurodegeneration.

Recently, there has been evidence suggesting similarities in tauopathy between NPC disease and Alzheimers disease (AD). The brains of NPC patients have been shown to have neurofibrillary tangles and neurodegeneration without amyloid β-protein (Aβ) deposits (13), which is believed to be responsible for promoting pathologies typically associated AD. The presence of neurofibrillary tangles is one of the diagnostic hallmarks of AD, and a major component of neurofibrillary tangles is hyperphosphorylated tau. Interestingly, Aβ adversely affects cellular cholesterol metabolism (23, 41), which in turn, induces tau phosphorylation in cultured neurons (42). The altered cholesterol metabolism in NPC1−/− brains and cells has also been shown to induce tau phosphorylation in NPC1−/− brains and cells (5, 19). Moreover, it has now been established that altered cholesterol metabolism is associated with the development of AD (43, 44), and that mitochondrial dysfunction is involved in the development of AD (45, 46). Therefore, it may be possible that AD and NPC share a common pathway involving cholesterol metabolism leading to neurodegeneration via mitochondrial dysfunction (44).

In conclusion, the present study has demonstrated that an elevation in the level of mitochondria membrane cholesterol, because of deficient NPC1 protein function, decreases cellular ATP levels causing impaired neurite outgrowth and enhanced susceptibility to oxygen radicals, which in turn is supposed to promote neurodegeneration in NPC1−/− mice. The addition of ATP can restore impaired neurite outgrowth and high susceptibility to neurotoxicity, which supports this notion. This information, suggesting that severe mitochondrial dysfunctions and subsequent decrease in cellular ATP levels may be the cause of neurodegeneration in NPC1 disease, provides a novel insight and direction for pursuing viable treatment options for NPC1 disease.

Acknowledgment—We thank Hitoshi Yamashita for helpful discussion.

REFERENCES

1. Patterson, M. C., Vanier, M. T., Suzuki, K., Morris, J. A., Carstea, E. D., Neufeld, E. B., Blanchette Mackie, E. J., and Pentchev, P. G. (2001) in *The Metabolic and Molecular Basis of Inherited Disease* (Scriver, C. R., Beaudet, A. L., Sly, W. S., and Valle, D., eds) pp. 3611–3633, McGraw-Hill Inc., New York
2. Liscum, L., Ruggiero, R. M., and Faust, J. R. (1989) *J. Cell Biol.* **108,** 1625–1636
3. Pentchev, P. G., Kruth, H. S., Comly, M. E., Butler, J. D., Vanier, M. T., Wenger, D. A., and Patel, S. (1986) *J. Biol. Chem.* **261,** 16775–16780
4. Kobayashi, T., Beuchat, M. H., Lindsay, M., Frias, S., Palmiter, R. D., Sakuraba, H., Parton, R. G., and Gruenberg, J. (1999) *Nat. Cell Biol.* **1,** 113–118
5. Sawamura, N., Gong, J. S., Garver, W. S., Heidenreich, R. A., Ninomiya, H., Ohno, K., Yanagisawa, K., and Michikawa, M. (2001) *J. Biol. Chem.* **276,** 10314–10319
6. Ribeiro, I., Marcao, A., Amaral, O., Sa Miranda, M. C., Vanier, M. T., and Millat, G. (2001) *Hum. Genet.* **109,** 24–32
7. Loftus, S. K., Morris, J. A., Carstea, E. D., Gu, J. Z., Cummings, C., Brown, A., Ellison, J., Ohno, K., Rosenfeld, M. A., Tagle, D. A., Pentchev, P. G., and Pavan, W. J. (1997) *Science* **277,** 232–235
8. Carstea, E. D., Morris, J. A., Coleman, K. G., Loftus, S. K., Zhang, D., Cummings, C., Gu, J., Rosenfeld, M. A., Pavan, W. J., Krizman, D. B., Nagle, J., Polymeropoulos, M. H., Sturley, S. L., Ioannou, Y. A., Higgins, M. E., Comly, M., Cooney, A., Brown, A., Kaneski, C. R., Blanchette-Mackie, E. J., Dwyer, N. K., Neufeld, E. B., Chang, T. Y., Liscum, L., Strauss, J. F., III, Ohno, K., Zeigler, M., Carmi, R., Sokol, J., Markie, D., O'Neill, R. R., van Diggelen, O. P., Elleder, M., Patterson, M. C., Brady, R. O., Vanier, M. T., Pentchev, P. G., and Tagle, D. A. (1997) *Science* **277,** 228–231
9. Liscum, L., and Klansek, J. J. (1998) *Curr. Opin. Lipidol.* **9,** 131–135
10. Neufeld, E. B., Wastney, M., Patel, S., Suresh, S., Cooney, A. M., Dwyer, N. K., Roff, C. F., Ohno, K., Morris, J. A., Carstea, E. D., Incardona, J. P., Strauss, J. F., 3rd, Vanier, M. T., Patterson, M. C., Brady, R. O., Pentchev, P. G., and Blanchette-Mackie, E. J. (1999) *J. Biol. Chem.* **274,** 9627–9635
11. Garver, W. S., Heidenreich, R. A., Erickson, R. P., Thomas, M. A., and Wilson, J. M. (2000) *J. Lipid Res.* **41,** 673–687
12. Wojtanik, K. M., and Liscum, L. (2003) *J. Biol. Chem.* **278,** 14850–14856
13. Suzuki, K., Parker, C. C., Pentchev, P. G., Katz, D., Ghetti, B., D'Agostino, A. N., and Carstea, E. D. (1995) *Acta Neuropathol.* **89,** 227–238
14. Love, S., Bridges, L. R., and Case, C. P. (1995) *Brain* **118,** 119–129
15. Auer, I. A., Schmidt, M. L., Lee, V. M., Curry, B., Suzuki, K., Shin, R. W., Pentchev, P. G., Carstea, E. D., and Trojanowski, J. Q. (1995) *Acta Neuropathol.* **90,** 547–551
16. Morris, M. D., Bhuvaneswaran, C., Shio, H., and Fower, S. (1982) *Am. J. Pathol.* **108,** 140–149
17. Higashi, Y., Murayama, S., Pentchev, P. G., and Suzuki, K. (1993) *Acta Neuropathol.* **85,** 175–184
18. Bu, B., Li, J., Davies, P., and Vincent, I. (2002) *J. Neurosci.* **22,** 6515–6525
19. Sawamura, N., Gong, J. S., Chang, T. Y., Yanagisawa, K., and Michikawa, M. (2003) *J. Neurochem.* **84,** 1086–1096
20. Walkley, S. U., Siegel, D. A., Dobrenis, K., and Zervas, M. (1998) *Ann. N. Y. Acad. Sci.* **845,** 188–199
21. Liu, Y., Wu, Y. P., Wada, R., Neufeld, E. B., Mullin, K. A., Howard, A. C., Pentchev, P. G., Vanier, M. T., Suzuki, K., and Proia, R. L. (2000) *Hum. Mol. Genet.* **9,** 1087–1092
22. Griffin, L. D., Gong, W., Verot, L., and Mellon, S. H. (2004) *Nat. Med.* **10,** 704–711
23. Michikawa, M., Gong, J. S., Fan, Q. W., Sawamura, N., and Yanagisawa, K. (2001) *J. Neurosci.* **21,** 7226–7235
24. Gong, J. S., Kobayashi, M., Hayashi, H., Zou, K., Sawamura, N., Fujita, S. C., Yanagisawa, K., and Michikawa, M. (2002) *J. Biol. Chem.* **277,** 29919–29926
25. Schnaitman, C., and Greenawalt, J. W. (1968) *J. Cell Biol.* **38,** 158–175
26. Wang, X., Liu, Z., Eimerl, S., Timberg, R., Weiss, A. M., Orly, J., and Stocco, D. M. (1998) *Endocrinology* **139,** 3903–3912
27. Sottocasa, G. L., Kuylenstierna, B., Ernster, L., and Bergstrand, A. (1967) *J. Cell Biol.* **32,** 415–438
28. Trumpower, B. L., and Edwards, C. A. (1979) *J. Biol. Chem.* **254,** 8697–8706
29. Zheng, X., Shoffner, J. M., Lott, M. T., Voljavec, A. S., Krawiecki, N. S., Winn, K., and Wallace, D. C. (1989) *Neurology* **39,** 1203–1209
30. Salvioli, S., Ardizzoni, A., Franceschi, C., and Cossarizza, A. (1997) *FEBS Lett.* **411,** 77–82
31. Ricquier, D., Casteilla, L., and Bouillaud, F. (1991) *FASEB J.* **5,** 2237–2242
32. Mattson, M. P., and Partin, J. (1999) *J. Neurosci. Res.* **56,** 8–20
33. Skladchikova, G., Ronn, L. C., Berezin, V., and Bock, E. (1999) *J. Neurosci. Res.* **57,** 207–218
34. Calanni Rindina, F., Baracca, A., Solaini, G., Rabbi, A., and Parenti Castelli, G. (1986) *FEBS Lett.* **198,** 353–356
35. Yao, P. M., and Tabas, I. (2001) *J. Biol. Chem.* **276,** 42468–42476
36. Colell, A., Garcia-Ruiz, C., Lluis, J. M., Coll, O., Mari, M., and Fernandez-Checa, J. C. (2003) *J. Biol. Chem.* **278,** 33928–33935
37. Shiao, Y. J., Lupo, G., and Vance, J. E. (1995) *J. Biol. Chem.* **270,** 11190–11198
38. Kuge, O., and Nishijima, M. (2003) *J. Biochem. (Tokyo)* **133,** 397–403
39. Garver, W. S., Krishnan, K., Gallagos, J. R., Michikawa, M., Francis, G. A., and Heidenreich, R. A. (2002) *J. Lipid Res.* **43,** 579–589
40. Garren, L. D., Gill, G. N., Masui, H., and Walton, G. M. (1971) *Recent Prog. Horm. Res.* **27,** 433–478
41. Gong, J. S., Sawamura, N., Zou, K., Sakai, J., Yanagisawa, K., and Michikawa, M. (2002) *J. Neurosci. Res.* **70,** 438–446
42. Fan, Q. W., Yu, W., Senda, T., Yanagisawa, K., and Michikawa, M. (2001) *J. Neurochem.* **76,** 391–400
43. Simons, M., Keller, P., Dichgans, J., and Schulz, J. B. (2001) *Neurology* **57,** 1089–1093
44. Michikawa, M. (2003) *J. Neurosci. Res.* **72,** 141–146
45. Hirai, K., Aliev, G., Nunomura, A., Fujioka, H., Russell, R. L., Atwood, C. S., Johnson, A. B., Kress, Y., Vinters, H. V., Tabaton, M., Shimohama, S., Cash, A. D., Siedlak, S. L., Harris, P. L., Jones, P. K., Petersen, R. B., Perry, G., and Smith, M. A. (2001) *J. Neurosci.* **21,** 3017–3023
46. Lustbader, J. W., Cirilli, M., Lin, C., Xu, H. W., Takuma, K., Wang, N., Caspersen, C., Chen, X., Pollak, S., Chaney, M., Trinchese, F., Liu, S., Gunn-Moore, F., Lue, L. F., Walker, D. G., Kuppusamy, P., Zewier, Z. L., Arancio, O., Stern, D., Yan, S. S., and Wu, H. (2004) *Science* **304,** 448–452

THE JOURNAL OF BIOLOGICAL CHEMISTRY VOL. 280, NO. 52, pp. 42759–42765, December 30, 2005

Cholesterol-mediated Neurite Outgrowth Is Differently Regulated between Cortical and Hippocampal Neurons*[S]

Received for publication, August 19, 2005, and in revised form, October 24, 2005 Published, JBC Papers in Press, November 2, 2005, DOI 10.1074/jbc.M509164200

Mihee Ko, Kun Zou, Hirohisa Minagawa, Wenxin Yu, Jian-Sheng Gong, Katsuhiko Yanagisawa, and Makoto Michikawa[1]

From the Department of Alzheimer's Disease Research, National Institute for Longevity Sciences, 36-3 Gengo, Morioka, Obu, Aichi 474-8522, Japan

The acquisition of neuronal type-specific morphogenesis is a central feature of neuronal differentiation and has important consequences for region-specific nervous system functions. Here, we report that the cell type-specific cholesterol profile determines the differential modulation of axon and dendrite outgrowths in hippocampal and cerebral cortical neurons in culture. The extent of axon and dendrite outgrowths is greater and the polarity formation occurs earlier in cortical neurons than in hippocampal neurons. The cholesterol concentrations in total homogenate and the lipid rafts from hippocampal neurons are significantly higher than those from cortical neurons. Cholesterol depletion by β-cyclodextrin markedly enhanced the neurite outgrowth and accelerated the establishment of neuronal polarity in hippocampal neurons, which were similarly observed in nontreated cortical neurons, whereas cholesterol loading had no effects. In contrast, both depletion and loading of cholesterol decreased the neurite outgrowths in cortical neurons. The stimulation of neurite outgrowth and polarity formation induced by cholesterol depletion was accompanied by an enhanced localization of Fyn, a Src kinase, in the lipid rafts of hippocampal neurons. A concomitant treatment with β-cyclodextrin and a Src family kinase inhibitor, PP2, specifically blocked axon outgrowth but not dendrite outgrowth (both of which were enhanced by β-cyclodextrin) in hippocampal neurons, suggesting that axon outgrowth modulated by cholesterol is induced in a Fyn-dependent manner. These results suggest that cellular cholesterol modulates axon and dendrite outgrowths and neuronal polarization under culture conditions and also that the difference in cholesterol profile between hippocampal and cortical neurons underlies the difference in neurite outgrowth between these two types of neurons.

Neurons contain two types of processes, axons and dendrites, which are structurally and functionally distinct and play different roles in the maintenance of brain functions. There are studies showing the significant role of lipids in the formation of neuronal polarity; it has been shown that phospholipids regulate neurite outgrowth in cultured neurons (1) and that the correct distribution of axonal membrane proteins requires the formation of sphingomyelin/cholesterol-rich microdomains, lipid rafts, and the maturation of the axonal plasma membrane requires the up-regulation of sphingomyelin synthesis (2, 3). Cholesterol also plays a prominent role in raft-mediated trafficking and sorting, because cholesterol depletion by methyl-β-cyclodextrin impedes trafficking from the trans-Golgi network to the apical membrane (4). It has been shown that cholesterol modulates dendrite outgrowth (5), that its deficiency enhances phosphorylation of tau and axonal depolymerization (6), and that axonal regeneration is dependent on local cholesterol reutilization *in vivo* (7). In addition, cholesterol supplied as glial lipoproteins stimulates the axon outgrowth of central nervous system neurons (8, 9). Moreover, previous studies have shown that glia-derived cholesterol is essential for synaptogenesis and synaptic plasticity (10, 11). These lines of evidence suggest that membrane lipids play essential roles in neurite outgrowth and the formation of synapse neuronal polarity.

The region-specific difference in the development of Alzheimer disease pathologies is known. For example, the initial amyloid-β protein deposition occurs in poorly myelinated areas of the basal neocortex and spreads into adjoining areas and the hippocampus, whereas the formation of neurofibrillary tangles, which contain hyperphosphorylated tau, preferentially occurs in the transentorhinal region and hippocampus in the absence of amyloid deposits (12–14). Previous studies have suggested that the altered cholesterol metabolism is associated with the development of Alzheimer disease (for review, see Ref. 15) via the modulation of amyloid-β synthesis (16, 17). Other lines of evidence suggest that cholesterol plays essential roles in the modulation of tau phosphorylation (6, 18, 19), neurofibrillary tangle formation (20), and neuronal survival (21, 22). These lines of evidence suggest that Alzheimer disease pathologies preferentially developing in specific brain regions may be explained by a region-specific difference in the lipid profile. However, the region-specific profiles of lipids in neurons and their effects on neuronal functions remain to be clarified. The present study was designed to determine whether there is any difference in the profiles of lipids in primary cultured neurons isolated from different regions, namely, the mouse cerebral cortices and hippocampus, and whether neuronal function, including neurite outgrowth and polarity formation, is modulated by cellular lipids.

MATERIALS AND METHODS

Cell Culture—Neuron-rich cultures were prepared from the cerebral cortices and hippocampi of rat brains on embryonic day 18. The isolated cerebral cortices and hippocampi were incubated in 2 ml of Hepes-buffered saline solution containing 0.25% trypsin-EDTA for 20 min at 37 °C. The tissues were then washed three times in Dulbecco's modified Eagle's medium (DMEM)[2] containing 10% fetal bovine serum. The tissues in 1 ml of DMEM containing 10% fetal bovine serum were sub-

* This work was supported by Grants H14-10 (Comprehensive Research on Aging and Health) and H17-004 (Research on Human Genome and Tissue Engineering) from the Ministry of Health, Labor, and Welfare of Japan and by the Program for Promotion of Fundamental Studies in Health of the National Institute of Biomedical Innovation, Japan. The costs of publication of this article were defrayed in part by the payment of page charges. This article must therefore be hereby marked "*advertisement*" in accordance with 18 U.S.C. Section 1734 solely to indicate this fact.

[S] The on-line version of this article (available at http://www.jbc.org) contains supplemental Figs. S1 and S2 and Experimental Procedures.

[1] To whom correspondence should be addressed. Tel.: 81-562-46-2311; Fax: 81-562-46-8569; E-mail: michi@nils.go.jp.

[2] The abbreviations used are: DMEM, Dulbecco's modified Eagle's medium; PBS, phosphate-buffered saline; β-CD, methyl-β-cyclodextrin; Mes, 4-morpholineethanesulfonic acid.

jected to gentle pipetting using a micropipette (Gilson) 10 times and to further pipetting using a fire-polished glass Pasteur pipette 10 times. The volume of solution containing dissociated tissues was adjusted to 10 ml by adding DMEM containing 10% fetal bovine serum, and the tissues were obtained as pellets by centrifugation at 800 rpm for 5 min. The samples were washed two times in DMEM by centrifugation at 800 rpm for 5 min. The dissociated cells were suspended in feeding medium (consisting of DMEM/F12 (50:50%) nutrient mixture and N_2 supplements) and plated onto poly-D-lysine-coated 12-well plates at a cell density of $5 \times 10^3/cm^2$. More than 99% of the cultured cells were identified as neurons by immunocytochemical analysis using a monoclonal antibody against microtubule-associated protein 2, a neuron-specific marker, on day 3 of culture (21).

Morphological Analysis—The cultured neurons were washed three times in PBS and incubated in PBS containing 4% paraformaldehyde for 15 min at room temperature. The cells were then washed three times in PBS and incubated in PBS containing 0.2% Triton X-100 and 1% bovine serum albumin for 15 min at room temperature. The cells were washed three times in PBS and incubated with a monoclonal anti-β-tubulin antibody (Covance, Berkeley, CA) at 2 μg/ml overnight at 4 °C. The cultured cells were then washed in PBS three times, and the anti-β-tubulin antibody bound to neuronal β-tubulin was visualized using an ABC kit (Vector Laboratories, Burlingame, CA). The photographs of stained neurons were captured using a charge-coupled device camera (DC500) (Leica Microsystems GMBH, Wetzar, Germany) attached to a phase-contrast microscope (Olympus IX70, Olympus Co., Ltd., Tokyo, Japan). The length of axons and dendrites/cell and the ratio of neurite number/cell were determined using an image analyzer (KS400, Karl Zeiss Co., Ltd., Jena, Germany). Longest-axon length, axonal plexus length, and total dendrite length are defined in supplemental Fig. S1.

Lipid Analysis—For the extraction of cellular lipids, dried cells were incubated in hexane:isopropanol (3:2 v/v) for 1 h at room temperature. The solvent in each plate was collected and dried under N_2 gas. The organic phases were redissolved in 400 μl of chloroform, and a 150-μl sample was transferred onto 96-well polypropylene plates (Corning Coster, Corning, NY) and dried under air flow. The dried lipids were then dissolved in 20 μl of isopropanol. The concentration of cholesterol was determined using a cholesterol determination kit, LTCII (Kyowa Medex, Tokyo), and the concentration of phospholipids was determined using a phospholipid determination kit, PLB (Wako, Osaka, Japan) as described previously (23).

Immunoblot Analysis—Immunoblot analysis was performed as described previously (18). The primary antibodies used were mouse monoclonal antibodies, Fyn sc-434 (1: 1,000 dilution, Santa Cruz Biotechnology, Inc.), flotillin (1:1000 dilution, BD Biosciences), and NCAM (1:1000 dilution, Chemicon International, Inc.). GM1 was detected using cholera toxin B-conjugated horseradish peroxidase (1:10,000, Sigma-Aldrich). After rinsing and incubation in the presence of an appropriate peroxidase-conjugated secondary antibody, the bands were detected with an ECL kit (Amersham Biosciences). Protein concentrations were determined using the bicinchoninic acid protein assay kit (Pierce).

Cholesterol Depletion and Drug Treatment—A stock solution of methyl-β-cyclodextrin (β-CD) (Sigma-Aldrich) was prepared by dissolving β-CD in DMEM/F12 medium at a concentration of 100 mM. For cholesterol depletion, neurons were treated with β-CD at a final concentration of 5 mM for 10 min at 37 °C, washed in the culture medium three times, and then cultured further for 5, 24, or 48 h. Cholesterol (Sigma-Aldrich) and PP2 (Calbiochem) were dissolved in 100% ethanol to prepare stock solutions at concentrations of 7 mg/ml and 5 mM, respectively. Cholesterol and PP2 solutions were diluted and used at final concentrations of 7 μg/ml and 5 μM, respectively.

Lipid Raft Fractions—Sucrose gradients were prepared by established methods with modifications (24, 25). Neurons were rinsed with PBS and scraped and homogenized with 1 ml of Mes-buffered saline (25 mM Mes, pH 6.5, 0.15 M NaCl) containing 1% Triton X-100, a mixture of protease inhibitors, Complete™, and phosphatase inhibitors. Extracts containing 350 μg of proteins were subjected to sucrose gradient analysis. Gradients were centrifuged for 20 h at 44,800 rpm at 4 °C in a SW 50.1 rotor (Beckman Instruments). Fractions (400 μl) were collected sequentially starting from the top of the gradient. The extraction of lipids and the subsequent determination of the concentrations of cholesterol and phospholipid in each sample were carried out according to previously described methods (23).

Triton X-100-soluble and -insoluble Fractions—Cultured neurons (1×10^6 cells) were washed three times with ice-cold PBS and scraped in 200 μl of 1% Triton X-100 in Mes-buffered saline. Neurons were lysed by pipetting 10 times followed by ultrasonication for 5 min at a high level at 4 °C in a Bioruptor (Cosmo Bio, Tokyo). Triton X-100-soluble and -insoluble fractions were separated by centrifugation at 100,000 × *g* for 60 min using a TLA-100 rotor (Beckman Instruments). The resulting pellet (Triton X-100-insoluble fraction) was washed with PBS three times and resuspended in 100 μl of radioimmune precipitation assay buffer; the resultant supernatant was used in lipid analysis. The supernatant, *i.e.* the Triton X-100-soluble fraction, was used in lipid analysis.

Statistical Analyses—All statistical analyses were conducted using the StatView 5.0 software package (Abacus Concepts Inc., Berkeley, CA). The data are expressed as means ± S.E., and statistical significance was assessed by an analysis of variance followed by post-hoc Fisher's PLSD test. A value of $p < 0.05$ was considered statistically significant.

RESULTS

Differential Neurite Outgrowth in Cultured Neurons Prepared from the Hippocampi and Cortices of Rat Embryos—Primary neurons were prepared from the hippocampi and cortices of rat embryos on embryonic day 18 and maintained for 1, 3, and 5 days in serum-free N_2-supplemented culture medium. The cultures were then stained with the anti-β-tubulin antibody. Cortical neurons immunostained with the anti-tubulin antibody on culture days 1, 3, and 5 are shown in Fig. 1, *a*, *c*, and *e*, respectively. Hippocampal neurons immunostained with the same antibody on culture days 1, 3, and 5 are shown in Fig. 1, *b*, *d*, and *f*, respectively. Cortical neurons had longer axons and dendrites than hippocampal neurons at each time point examined. The longest-axon length, axonal plexus length, dendrite length, and number of neurites were determined as described under "Materials and Methods" (see also supplemental Fig. S1). The longest-axon length and total dendrite length were greater in cortical neurons than in hippocampal neurons; these lengths increased with culture time in both types of neurons (Fig. 1, *g* and *i*). The axonal plexus length of cortical neurons on culture day 5 was greater than that of hippocampal neurons (Fig. 1*h*). In contrast, the number of neurites per cortical neuron on culture day 5 was similar to the number of neurites per hippocampal neuron (Fig. 1*j*).

Differential Lipid Profiles in Cultured Neurons Prepared from the Hippocampi and Cortices of Rat Embryos—We next determined the concentrations of cholesterol and phospholipids in these neurons. The cholesterol concentration in hippocampal neurons was significantly higher than in cortical neurons (Fig. 2*a*); however, the concentration of phospholipids was similar between these two types of neurons (Fig. 2*b*). The concentrations of cholesterol and phospholipids in Triton X-100-soluble and -insoluble fractions in each neuronal culture were also

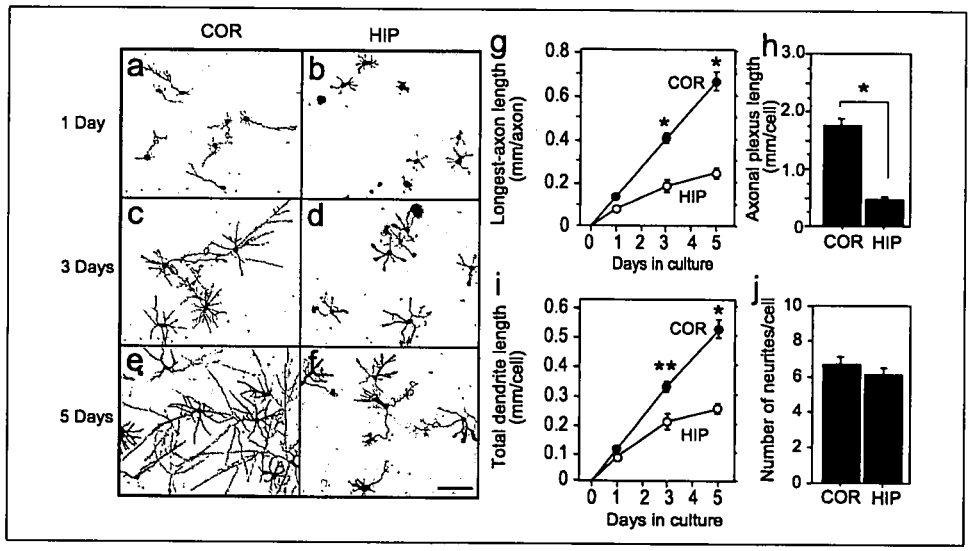

FIGURE 1. **Difference in neurite outgrowth between cortical and hippocampal neurons in culture.** Primary neurons were prepared from cortices and hippocampi of rat brains on embryonic day 18 and plated on poly-D-lysine-coated 12-well plastic plates at a cell density of 5×10^3/well. *a–f*, the neurons were cultured in serum-free N_2-supplemented medium (N_2-medium) and fixed and immunostained with anti-β-tubulin antibody on the days indicated. *Scale bar* represents 100 μm. *COR* and *HIP* represent cortical neurons and hippocampal neurons, respectively. Neurons from stages 3–5 (26) were analyzed. Longest-axon length (*g*) and total dendrite length (*i*) per neuron on days 1, 3, and 5 in culture were determined. Axonal plexus length (*h*) and number of neurites (*j*) per neuron were determined on culture day 5. The number of neurons analyzed was 25 in each culture. *, $p < 0.0001$, and **, $p < 0.005$, between cortical and hippocampal neurons. Four independent experiments showed similar results.

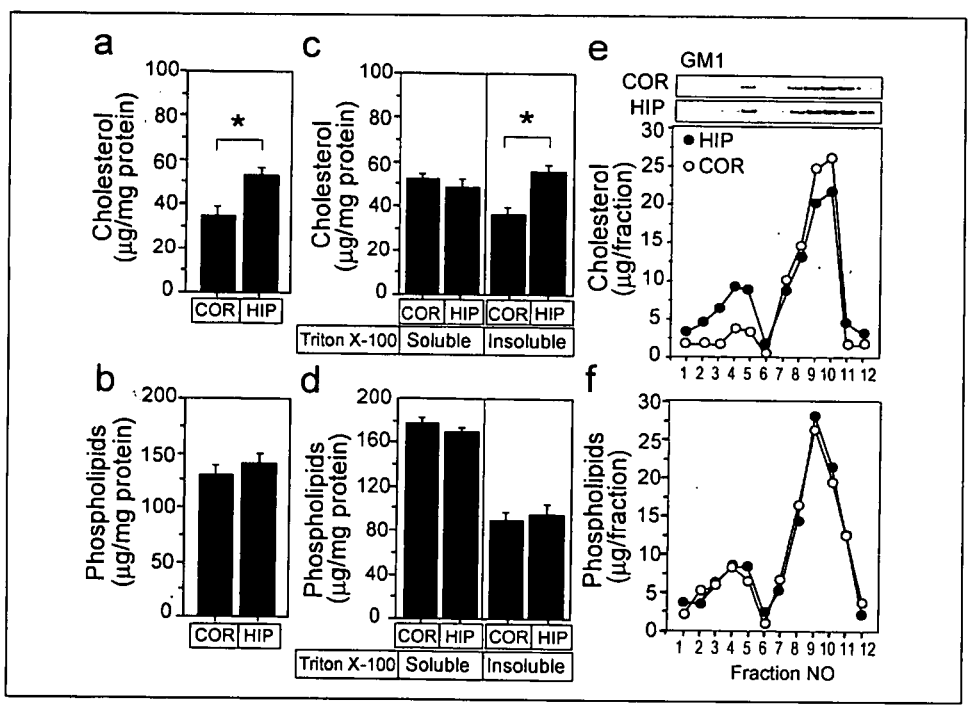

FIGURE 2. **Characterization of lipid profiles of cortical and hippocampal neurons.** Cholesterol and phospholipid concentrations in cortical and hippocampal neurons cultured in N_2-medium for 5 days were analyzed as described under "Materials and Methods." The concentrations of cholesterol (*a*) and phospholipids (*b*) in hippocampal (*HIP*) and cortical (*COR*) neurons per mg of protein were determined. In addition, the concentrations of cholesterol (*c*) and phospholipids (*d*) in the Triton X-100-soluble and -insoluble fraction from hippocampal and cortical neurons were determined. The data represent mean ± S.E. The number of samples was six for each treatment. *, $p < 0.05$. Three independent experiments showed similar results. Isolation of lipid raft fractions from cultured hippocampal and cortical neurons was performed by sucrose density gradient ultracentrifugation, and cholesterol (*e*) and phospholipid (*f*) levels in each fraction are shown.

determined. The cholesterol concentration in the Triton X-100-insoluble fraction from hippocampal neurons was higher than that from cortical neurons, whereas the concentration in the Triton X-100-soluble fraction from hippocampal neurons was similar to that from cortical neurons (Fig. 2*c*). There were no significant differences in the concentrations of phospholipids in the Triton X-100-soluble and -insoluble fractions between hippocampal and cortical neurons (Fig. 2*d*). Because cholesterol concentration in the Triton X-100-insoluble fraction was different between these two types of neurons, we next examined lipid distribution in the lipid raft fractions. The lipid raft fractions were isolated as described under "Materials and Methods." The cholesterol concentration in the lipid raft fractions isolated from hippocampal neurons was higher than that from cortical neurons (Fig. 2*e*), whereas there was no significant difference in phospholipid concentration between these two types of neurons in culture (Fig. 2*f*).

Cholesterol Concentration-dependent Regulation of Neurite Outgrowth in Hippocampal and Cortical Neurons—To determine whether a higher cholesterol concentration is responsible for the shorter neurite outgrowth from hippocampal neurons than from cortical neurons, cholesterol concentration in both types of neurons was modulated by treatment with β-cyclodextrin and cholesterol. Interestingly, cholesterol depletion by β-cyclodextrin stimulated neurite outgrowth in hippocampal neurons (Fig. 3, *b* and *d*), which made these neurons similar to cortical neurons without treatment (Fig. 3, *a* and *d*). In contrast, β-cyclodextrin treatment decreased the extent of neurite outgrowth in cortical neurons (Fig. 3, *a* and *c*). Cholesterol loading also decreased the extent of neurite outgrowth in cortical neurons (Fig. 3, *a* and *e*), whereas it had no effects on neurite outgrowth in hippocampal neurons (Fig. 3, *b* and *f*). Neuronal development in cultures has been defined from stages 1 to 5 (26). On the basis of these criteria, we determined the ratio of

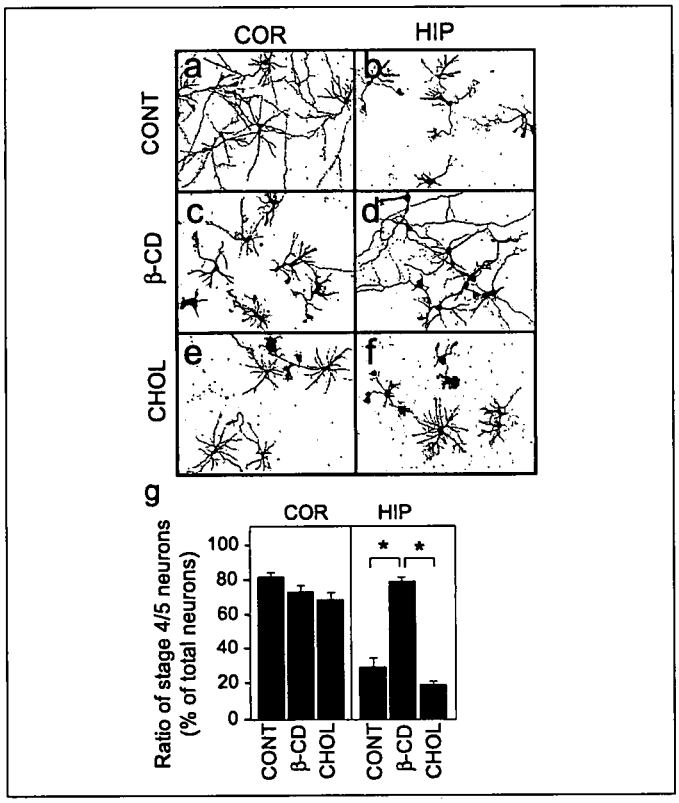

FIGURE 3. **Cholesterol-dependent neurite outgrowth and polarity formation in cortical and hippocampal neurons.** Cortical (*COR*) and hippocampal neurons (*HIP*) were maintained in N_2-medium for 3 days; each culture was treated with β-CD at 5 mM for 10 min, washed in N_2-medium three times, and maintained for another 2 days. Cultures maintained for 3 days were treated with cholesterol (*CHOL*) at 7 μg/ml and maintained for another 2 days. The neurons were then fixed and processed for immunocytochemistry using the anti-tubulin antibody (*a–f*). The ratio of stage 4 and 5 neurons to total neurons in cortical and hippocampal neurons was determined (*g*). The data represent mean ± S.E. For each treatment, 250 neurons were counted. *, $p < 0.0001$. Three independent experiments showed similar results. *CONT*, control.

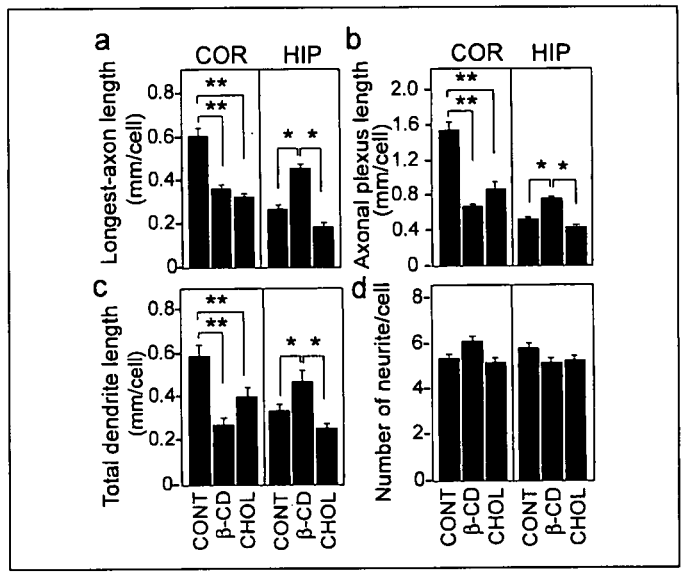

FIGURE 4. **Cholesterol-dependent modulation of axon and dendrite outgrowths in cortical and hippocampal neurons in culture.** Cultured neurons were maintained in N_2-medium for three days after plating, and the cultures were treated with β-CD or cholesterol (*CHOL*) as described in the legend for Fig. 3. The neurons were then immunostained with the anti-tubulin antibody, and longest-axon length (*a*), axonal plexus length (*b*), total dendrite length (*c*), and number of neurites (*d*) per cell were determined. *COR* and *HIP* represent cortical and hippocampal neurons, respectively. The data represent mean ± S.E. Twenty-five neurons were counted for each treatment. *, $p < 0.005$; **, $p < 0.0001$. Three independent experiments showed similar results. *CONT*, control.

neurons at stages 4 and 5 to the total number of neurons. As shown in Fig. 3*g*, cholesterol depletion by β-cyclodextrin treatment or cholesterol loading had no significant effects on the development of cortical neurons (*left panel*). In contrast, β-cyclodextrin treatment stimulated the development of hippocampal neurons; however, cholesterol loading had no significant effects (Fig. 3*g*, *right panel*).

The effects of cholesterol depletion and loading on longest-axon length, axonal plexus length, and total dendrite length of cortical andhippocampal neurons were determined. Cholesterol depletion by treatment with β-cyclodextrin and cholesterol loading decreased the longest-axon length, axonal plexus length, and total dendrite length of cortical neurons (Fig. 4, *a–c*, respectively). In contrast, cholesterol depletion by treatment with β-cyclodextrin increased the longest-axon length, axonal plexus length, and total dendrite length of hippocampal neurons (Fig. 4, *a–c*, respectively), whereas cholesterol loading had no significant effects on these three parameters in hippocampal neurons (Fig. 4, *a–c*). In both types of neurons, these chemicals had no effects on neurite numbers (Fig. 4*d*).

Cholesterol concentrations in cultured neurons treated with β-cyclodextrin or cholesterol loading were determined. Cholesterol concentration in neurons was reduced at 5 h and was recovered at 24 h following treatment with β-cyclodextrin in both cortical and hippocampal neurons (Fig. 5*a*). Cholesterol concentration in neurons increased at 24 h following treatment with cholesterol in both cortical and hippocampal neurons (Fig. 5*a*), although phospholipid concentrations remained unchanged by these treatments (Fig. 5*a*). We further determined the longest-axon length, total dendrite length, and neurite length per cell in cortical and hippocampal neurons treated with β-CD or cholesterol. As shown in Fig. 5*b*, the neurite length was dependent on the treatments.

Fyn, a Member of the Src Family, in Lipid Raft Fraction Is a Key Molecule Modulating Cholesterol-dependent Axon Outgrowth—The observations mentioned above suggest that the difference in cholesterol concentration between cortical and hippocampal neurons could explain differences in neurite outgrowth and neuronal development between these two types of neurons. Because cholesterol concentrations differ in the Triton X-100-insoluble fraction and the lipid raft fraction but not in the Triton X-100-soluble fraction between these two types of neurons (Fig. 2), proteins that are localized in lipid rafts and also play a role in axon and dendrite outgrowths may underlie these differences between cortical and hippocampal neurons in terms of neurite outgrowth. Among the molecules examined, only the level of Fyn in the raft fraction was significantly high in hippocampal neurons treated with β-cyclodextrin, whereas that in total homogenates did not alter (Fig. 6*a*). The levels of flotillin and GM1 did not differ between cortical and hippocampal neurons following these treatments (Fig. 6*a*).

We next determined whether an inhibitor of Fyn signaling, PP2, inhibits the cholesterol deficiency-induced stimulation of axon and dendrite outgrowths in hippocampal neurons. The treatment of hippocampal neurons with 5 μM PP2 inhibited enhanced neurite outgrowth induced by β-cyclodextrin (Fig. 6*b*). However, PP2 did not have any effects on neurite growth in control and cholesterol-loaded neurons (Fig. 6*b*). The neurite outgrowth in hippocampal neurons treated with β-cyclodextrin or cholesterol in the presence or absence of PP2 was quantified. The treatment of hippocampal neurons with PP2 significantly inhibited the increase in longest-axon length and axonal plexus length induced by β-cyclodextrin (Fig. 6*c*, *black bars*); however, PP2 had no effect on neurite outgrowth in control neurons and cholesterol-loaded neurons (Fig. 6*c*, *white bars*). An inhibitory effect of PP2 on the